SI Experimental Procedures

Construct design

The BG505, B41, and ZM197M SOSIP.664 constructs have been described elsewhere (Julien et al., 2015; Pugach et al., 2015; Sanders et al., 2013). The AMC008 *env* gene is derived from a subtype B virus, isolated 8 months post-seroconversion from an individual in the Amsterdam Cohort Studies on HIV/AIDS who eventually developed broadly neutralizing antibodies (patient H18818 in (Euler et al., 2010)). The AMC008 SOSIP.664 gp140 construct was designed as previously described (Julien et al., 2015; Pugach et al., 2015; Sanders et al., 2013), by introducing the following sequence changes: A501C and T605C (gp120-gp41$_{ECTO}$ disulfide bond; (Binley et al., 2000)); I559P in gp41$_{ECTO}$ (trimer-stabilizing; (Sanders et al., 2002)); REKR to RRRRRR in gp120 (cleavage enhancement; (Binley et al., 2002)); a stop codon at gp41$_{ECTO}$ residue 664 (improvement of homogeneity and solubility; (Klasse et al., 2013)). SOSIP.664-D7324 trimers contain a D7324 epitope-tag sequence at the C-terminus of gp41$_{ECTO}$ and were made by adding the amino-acid sequence GSAPTKAKRRVVQREKR after residue 664 in gp41$_{ECTO}$ (Sanders et al., 2013). Similarly, biotinylated SOSIP.664-aviB trimers were generated by adding the avidin (avi) sequence GLNDIFEAQKIEWHE after residue 664, followed by biotinylation (aviB) as described (Sok et al., 2014). Point mutants were made by Quikchange site directed mutagenesis (Agilent, Stratagene), and verified by sequencing. All experiments used D7324-tagged trimers, except for DLS, SAXS, HDX-MS and ITC studies (untagged trimers), SPR (His-tagged trimers) and Octet assays (aviB-tagged trimers).

Construction of an AMC008-LAI chimeric molecular clone

The molecular clone of LAI was used as the backbone to construct a chimeric virus (Peden et al., 1991). This LAI clone contains a unique Sal1 restriction site 434 nucleotides upstream of the *env* start codon and a unique BamH1 site at the codons specifying amino acids G751 and S752 in LAI gp160 (HXB2 numbering). A DNA fragment was synthesized that contained the LAI sequences between the Sal1 site and the *env* start codon, followed by the AMC008 *env* sequence up to the BamH1 site

(Genscript). The fragment was then cloned into the LAI molecular clone backbone using Sal1 and BamH1 as digestion enzymes. The resulting molecular clone encodes the complete AMC008 gp160 sequence, except for the C-terminal 106 amino acids of the cytoplasmic tail, which are derived from LAI gp160. The authenticity of the clone was verified by sequencing. Infectious virus was produced from the clone by transfection and used in virus infectivity and neutralization assays based on TZM-bl cells as described below. When the neutralization-sensitivity of the AMC008 –LAI chimeric virus was assessed using a panel of human sera and MAbs and a panel of test viruses at the Duke University Medical Center, it was classified as being in Tier-1B (not shown). Note that the various AMC008 SOSIP.664 constructs are based on the same *env* sequence that is present in the AMC008 chimeric molecular clone.

Env protein expression

Proteins encoded by the various *env* genes described above were expressed in adherent 293T cells, or in 293F or 293S ($GnTI^{-/-}$) variants adapted for suspension cultures, essentially as described (Julien et al., 2013; Sanders et al., 2013). All experiments with purified trimers used 293F cell-expressed proteins, except for ITC assays when the producer cell was, in most cases, 293S. The 293T or 293S cells were maintained in Dulbecco's modified Eagle's medium (DMEM) supplemented with 10% fetal calf serum (FCS), penicillin (100 U/ml) and streptomycin (100 µg/ml). For trimer expression on a small-scale, 293T cells were seeded at a density of 5.5×10^4/ml in a 6-well plate. The next day, when the cells had reached a density of 1.0×10^6/ml, they were transfected using polyethyleneimine (PEI), as previously described (Kirschner et al., 2006). Briefly, PEI-MAX (1.0 mg/ml) in water was mixed with expression plasmids for Env and Furin (Binley et al., 2000) in OPTI-MEM (Gibco). For one well, 3.75 µg of Env plasmid, 1.25 µg of Furin plasmid and 12.5 µl PEI-MAX (1mg/ml) were added in 3 ml of growth media (DMEM + 10% FCS + penicillin and streptomycin). Culture supernatants were harvested 72 h after transfection.

For larger-scale production, Env proteins were produced in 293F cells using a protocol similar to that described previously (Julien et al., 2013; Sanders et al., 2013). Briefly, PEI-MAX (1.0 mg/ml) in water was mixed with expression plasmids

for Env and Furin in OPTI-MEM. For cultures in a 2L disposable Nalgene flask (VWR), 250 µg of Env plasmid, 62.5 µg of Furin plasmid and 0.94 mg of PEI-MAX were added to 1L of pre-warmed Free-style 293 expression medium (Life Technologies). 293F cells were cultured for 6-7 days at 37°C, in an atmosphere containing 8% CO_2 and at a rotation speed of 125 rpm.

Trimer purification

Env proteins were purified from transfection supernatants by affinity chromatography using a PGT145- or a 2G12-column, essentially as described (Julien et al., 2013; Pugach et al., 2015; Sanders et al., 2013). The columns were made by coupling PGT145 or 2G12 to CNBr-activated Sepharose 4B beads (GE Healthcare). Briefly, supernatants were vacuum filtered through 0.2-µm filters and passed (0.5–1 ml/min flow rate) through the column, which was then washed with 2 column volumes of buffer (0.5 M NaCl, 20 mM Tris, pH 8.0). Bound Env proteins were eluted using 1 column volume of 3 M $MgCl_2$ and then immediately buffer-exchanged into 75 mM NaCl, 10 mM Tris, pH 8.0, using Vivaspin-20 tubes. The proteins were concentrated using Vivaspin columns with a 30-kDa cut off (GE Healthcare). 2G12-purified Env proteins were further fractionated by size exclusion chromatography (SEC) to obtain pure trimers, whereas the PGT145 column yielded pure trimers without the need for SEC. Protein concentrations were determined using UV_{280} absorbance and theoretical extinction coefficients via Expasy (ProtParam tool). All experiments were performed with PGT145-purified trimers except for ITC and Octet studies, which used 2G12/SEC-purified trimers.

Neutralization assays

The TZM-bl reporter cell line, which stably expresses high levels of CD4 and the co-receptors CCR5 and CXCR4 and contains the luciferase and β-galactosidase genes under the control of the HIV-1 long-terminal-repeat promoter, was obtained through the NIH AIDS Research and Reference Reagent Program, Division of AIDS, NIAID, NIH (John C. Kappes, Xiaoyun Wu, and Tranzyme Inc., Durham, NC).

TZM-bl cell neutralization assays using Env-pseudotyped or chimeric molecular clone viruses were performed at two different sites: DUMC, Duke University Medical Center, Durham, NC (for methodology see (Montefiori, 2009)); AMC, Academic Medical Center, Amsterdam (for methodology see (Sanders et al., 2013)). The assays at DUMC were performed essentially as described in protocols at: http://www.hiv.lanl.gov/content/nab-reference-strains/html/home.htm. Assays performed at AMC had the following modifications. For use in virus production, 293T cells (2×10^5) were seeded in a 6-well tissue culture plate (Corning) in 3 ml of DMEM (Gibco) containing 10% FCS, penicillin (Sigma) and streptomycin sulphate (Gibco) (both at 100 U/ml) per well. The culture was refreshed after 1 d by adding 3 ml of culture medium when the cells had reached a confluence of 90–95% and were ready for transfection. To make Env-pseudotyped viruses, the following expression plasmids were added to 240 µl of OPTI-MEM (Gibco) and 10 µl of lipofectamine 2000 (Invitrogen) per well: 1.6 µg of BG505.T332N Env plasmid and 2.4 µg of pSG3ΔEnv plasmid (obtained through the NIH AIDS Research and Reference Reagent Program, Division of AIDS, NIAID, NIH (John C. Kappes, Xiaoyun Wu, and Tranzyme Inc. Durham, NC)). To make infectious chimeric viruses by transfection the same procedure was used except that 4 µg of a molecular clone plasmid was added per well. After incubation for 20 min at room temperature, the transfection mixture was added to the cells, and the culture supernatants were harvested 48 h later as the source of Env-pseudotyped or infectious chimeric viruses for infection and/or neutralization experiments.

One day prior to virus infection, 1.7×10^4 TZM-bl cells per well were seeded in a 96-well plate in DMEM containing 10% FCS, 1× MEM nonessential amino acids, penicillin and streptomycin (both at 100 U/ml), and incubated at 37°C for 24h in an atmosphere containing 5% CO_2. To determine neutralization activity of rabbit sera, a fixed amount of virus (500 pg of p24-antigen equivalent) was incubated for 1 h at room temperature with heat-inactivated sera (3-fold serial dilutions starting at 1:20). The mix was then added to the cells in the presence of 40 µg/ml DEAE-Dextran (Sigma) and Saquinavir, in a total volume of 200 µl. Three days later, the medium was removed and the cells were washed once with PBS (150 mM NaCl, 50

mM sodium phosphate, pH 7.0) and lysed in Reporter Lysis Buffer (Promega). Luciferase activity was measured using a Luciferase Assay kit (Promega) and a Glomax Luminometer according to the manufacturer's instructions (Turner BioSystems). All infections were performed in duplicate. Uninfected cells were used to correct for background luciferase activity. To determine the V3 specificity of the NAb responses, sera were first incubated for 1 h at room temperature with 1mg/ml of a V3 peptide (BG505: TRPNNNTRKSIRIGPQAFYATGDIIGDIRQAH or AMC008: TRPNNNTRKSINIGPGRAFYTTGEIIGDIRQAH). The residual NAb titers were then quantified as described above. The infectivity of each virus in the absence of serum was set at 100%. Nonlinear regression curves were determined and the 50% inhibitory serum dose (ID_{50}) was calculated using a sigmoid function in Prism software version 5.0.

SDS-PAGE

Env proteins were analyzed using SDS-PAGE followed by western blotting or Coomassie blue dye staining (Sanders et al., 2002; Schülke et al., 2002). The input material was mixed with loading dye (25 mM Tris, 192 mM Glycine, 20% v/v glycerol, 4% m/v SDS, 0.1% v/v bromophenol blue in milli-Q water) and incubated at 95°C for 5 min prior to loading on a 4-12% or 8% Tris-Glycine gel (Invitrogen). For reducing SDS-PAGE, dithiothreitol (DTT; 100 mM) was included in the loading dye. The gels were run for 2h at 125 V (0.07 A) using 50 mM MOPS, 50 mM Tris, pH 7.7 as the running buffer (Invitrogen). Western blot analysis of SDS-PAGE gels using mouse MAb ARP3119 (1:2,000 dilution, i.e. 0.2 µg/ml), followed by HRP-labeled goat anti-mouse IgG (1:5000; Jackson Immunoresearch) was performed as previously described (Sanders et al., 2002). The Western Lightning ECL system (PerkinElmer Life Sciences) was used for luminometric detection. Coomassie blue staining of SDS-PAGE gels was performed using the PageBlue Protein Staining Solution (Thermo Scientific).

Blue Native-PAGE

For BN-PAGE (Sanders et al., 2002; Schülke et al., 2002), the input Env proteins were mixed with loading dye (500µl 20x MOPS Running Buffer (1M MOPS

+ 1M Tris, pH 7.7)+ 1000µl 100% Ultrapure Glycerol (Invitrogen cat#15514-011) + 50µl 5% Coomassie Brilliant Blue G-250 + 600µl milli-Q water) and directly loaded onto a 4–12% Bis-Tris NuPAGE gel. The gels were run for 1.5 h at 200 V (0.07 A) using Anode-Buffer (20x NativePAGE Running Buffer (Invitrogen) in milli-Q water) and Cathode-Buffer (1% NativePAGE Cathode-Buffer Additive in Anode-Buffer; both from Invitrogen). Western blot analysis of BN-PAGE gels was carried out using human MAb 2G12 (0.1 µg/ml), followed by HRP-labeled goat anti-human IgG (1:5,000 dilution, Jackson Immunoresearch and the Western Lightning ECL system (PerkinElmer Life Sciences), essentially as described previously (Sanders et al., 2002). BN-PAGE gels were stained using the Colloidal Blue Staining Kit (Life Technologies).

Surface plasmon resonance (SPR)

SPR was performed on a Biacore 3000 instrument at 25°C, using HBS-EP (10 mM HEPES [pH 7.4], 150 mM NaCl, 3 mM EDTA, 0.002% P20 surfactant) as the running buffer (GE Healthcare). The D7324 antibody (Aalto BioReagents) was coupled to the chip as previously described (Yasmeen et al., 2014), to an immobilization level of 9,000 resonance units (RU). The flow rate was adjusted to 10 µl/min. The ligands, i.e., D7324-tagged BG505 SOSIP.664, v4.1 and v4.2 trimers, diluted in running buffer to 20 µg/ml, were then captured, giving immobilization levels (R_L values) of 300 RU. A control channel into which no trimers were injected was used for background subtraction. In the simple binding assessment, the analytes, i.e., the test MAb or CD4-IgG2 (500 nM, diluted in HBS-EP), were allowed to associate with the trimers for 5 min before dissociation was recorded for 10 min. The flow rate was 50 µl/min throughout each run. After each cycle, the surface was regenerated by a 60 s injection of 10mM Glycine [pH 2.0], at a flow rate of 30 µl/min. Induction of conformational changes by CD4 was studied in the SPR format by injecting two analytes in a single cycle. The first analyte (CD4-IgG2; 500 nM) was injected for 200 s followed by the second (17b; 500 nM) for a further 200 s, both at a flow rate of 30 µl/min. After each cycle, the surface was regenerated as described above, before fresh trimer was captured for the next run.

D7324-capture ELISA

This method has been described elsewhere (Derking et al., 2015; Sanders et al., 2013). Microlon-600 96-well, half-area plates (Greiner Bio-One) were coated overnight with Ab D7324 at 10 μg/ml in 0.1 M $NaHCO_3$, pH 8.6 (50 μl/well). After washing and blocking steps, purified BG505 SOSIP.664-D7324 trimers were added at 2 μg/ml in TBS for 2 h. Unbound trimers were removed by 2 wash steps with TBS before various concentrations of test Abs were added for 2 h. After 3 washes with TBS, HRP-labeled goat anti-human IgG (Jackson Immunoresearch) was added at a 1:3000 dilution in TBS/2% skimmed milk for 1 h, followed by 5 washes with TBS/0.05% Tween-20. Colorimetric detection was performed using a solution containing 1% 3,3′,5,5′-tetramethylbenzidine (Sigma-Aldrich), 0.01% H_2O_2, 100 mM sodium acetate and 100 mM citric acid. Color development (absorption at 450 nm) was stopped using 0.8 M H_2SO_4 (25 μl) when a plateau value was reached in the two wells containing the highest Ab concentration. In some experiments (Fig. S1, Data S1), MAbs 17b or 412d were added to the immobilized Env proteins in the presence of two-domain sCD4 (1.0 μg/ml). In other experiments (Fig. S1H), a fixed concentration of 14e (0.1 μg/ml), 19b (0.6 μg/ml) or 39F (1.0 μg/ml) was incubated in solution with escalating concentrations of V3 peptides (Genscript) before adding the mixture to the ELISA plate. The V3 peptides (wild-type: CTRPNNNTRKSIRIGPQAFYATGDIIGDIRQAHC; A316W: CTRPNNNTRKSIRIGPGQWFYATGDIIGDIRQAHC) were cyclized by a disulfide bond between residues 1 and 35. To quantify antibody responses in immunized rabbits, sera (from week-22) were serially diluted in 3-fold steps from a 1:100 start point, using 40% sheep serum (Biotrading) and 2% milk powder in TBS as the buffer. When V3-directed Ab responses were analyzed, the sera were incubated in solution with a V3 peptide (1 μg/ml) for 1 h prior to adding the mixture to the test wells. The peptide sequences were identical to the V3 region of the immunogen. As with the BG505 V3 peptides described above, the peptides were cyclized by a disulfide bond between residues 1 and 35. The sequences of the AMC008 peptides were (wild-type: CTRPNNNTRKSINIGPGRAFYTTGEIIGDIRQAHC; A316W: CTRPNNNTRKSINIGPGRWFYTTGEIIGDIRQAHC. The secondary antibody was goat

anti-rabbit IgG (Jackson Immunoresearch), and the color development procedures were as described above.

V3 peptide ELISA

To determine V3 Ab responses in BG505-immunized mice and rabbits, 96-well MaxiSorp plates were coated with 2 μg/ml of a cyclized V3-peptide in PBS, by incubation overnight at 4°C. The V3 peptide was based on the BG505, AMC008 or B41 sequence, as appropriate, either unmodified or including the A316W change present in SOSIP.v4 trimers. The plates were then washed with PBS + 0.1% Tween-20 and blocked with PBS + 0.05% Tween-20 + 3.3% FBS + 2% BSA (PBS-TFB), for 1.5 h at room temperature. After washing, mouse or rabbit serum dilutions were added in PBS-TFB. The subsequent steps in the assay were as described for the D7324 capture ELISA for determining anti-trimer Ab titers, using either an HRP-labeled goat anti-mouse or an HRP-labeled goat anti-rabbit secondary antibody, as appropriate.

ELISA-based thermostability assay

As a screening assay for trimer stability, we devised a new thermal melting assay suitable for use on culture supernatants containing unpurified BG505 SOSIP.664-D7324 trimers (SI Fig. 1D-G). Supernatants (typically 60 μl containing ~15 μg/ml of total Env protein) were incubated for 30 min in a temperature gradient ranging from 39-77°C using a G-storm PCR machine (GRI Lab Care). The supernatants were then transferred to a 96-well plate and a D7324-capture ELISA was performed as described above. The 2G12 detection MAb was used at 0.1 μg/ml, a concentration that gives ~75% of the maximal signal in this ELISA format and, hence, allows any temperature-dependent loss of 2G12 reactivity to be quantified. When multiple, unpurified BG505 SOSIP.664-D7324 trimer variants were tested, the results from this screening assay correlated well with the outcome of DSC experiments using the same (but purified) trimers (Fig. S1G). However, the midpoints of thermal denaturation (T_m) in the present assay were consistently 3-5°C lower than obtained via DSC, probably because the 2G12 epitope unfolds or is perturbed at a lower temperature than the bulk of the trimer.

***Biolayer interferometry* (BLI)**

BLI assays were performed using the Octet Red96 instrument (Pall FortéBio). C-terminally His-tagged two-domain sCD4 (domains 1 and 2, expressed in 293F cells and purified via Ni-NTA affinity chromatography and SEC) was immobilized onto Dip and Read Ni-NTA-coated biosensors for 120 s followed by a 60 s baseline measurement in Kinetics Buffer (phosphate-buffered saline [PBS] pH 7.2 supplemented with 0.01% w/v bovine serum albumin and 0.002% v/v Tween 20). The probes were then dipped for 300 s into wells containing 200 nM of BG505 SOSIP.664-aviB wild-type or BG505 SOSIP.664-AviB containing single or double stabilizing mutations (E64K, H66R, A316W, version 4.1, or 4.2), in the same buffer. After the association step, the probes were placed into wells containing only the buffer for 600 s to measure dissociation. An inter-step correction was applied to align the end of the association curve to the beginning of the dissociation curve, and a single binding site model was used to determine on- and off-rates from the aligned curves.

Differential scanning calorimetry (DSC)

Thermal denaturation was studied using a nano-DSC calorimeter (TA instruments). All Env protein samples were first extensively dialyzed against PBS, and the protein concentration then adjusted to 0.1–0.3 mg/ml. After loading the sample into the cell, thermal denaturation was probed at a scan rate of 60°C/h. Buffer correction, normalization and baseline subtraction procedures were applied before the data were analyzed using NanoAnalyze Software v.3.3.0 (TA Instruments). The data were fitted using both two-state and non-two-state models, as the asymmetry of some of the peaks suggested that unfolding intermediates were present. We report the T_m values derived from the two-state model in the main text, while the multiple T_m values based on the non-two-state models are in the SI section. The DSC experiments were all performed with SOSIP.664-D7324 trimers, but we determined that the presence of the D7324-tag does not alter the T_m values

compared to the corresponding non-tagged trimers (data not shown). By running multiple DSC runs with the same protein (BG505 SOSIP.664-D7324), we determined that the standard deviation of the nano-DSC melting temperatures is +/- 0.3°C.

Dynamic light scattering (DLS)

DLS measurements were performed at 20°C using a Dynapro Nanostar instrument (Wyatt Technologies), with 40 acquisitions of 5 s each. Each sample was spun at 10,000 x g for 10 min prior to the DLS measurement to remove any trace aggregates or dust from the sample. The hydrodynamic radius (R_h) and the molecular weight (MW) were calculated using the Dynamics Analysis software (Wyatt Technologies), assuming a spherical model. To determine the Rh of stabilized SOSIP.664 trimers more precisely, we opted for DLS instead of the SEC/quasi-elastic light scattering (QELS) method used previously (Julien et al., 2013). The reason is that the use of flow mode SEC coupled to static and QELS detectors is limited by fitting using a mono-modal model. Calculated Rh values derived from this method thus represent the mean and distribution of diffusion constants. For a protein sample containing a small amount of polydispersity that is attributable to the presence of larger species, the resulting Rh value can be artificially elevated. As some preparations of BG505 SOSIP.664 trimers can contain up to ~5% of higher-order aggregates that are not completely separated from the trimer by SEC, their presence may account for the higher Rh values (i.e. 8.1 nm for the BG505 SOSIP.664 trimer (Julien et al., 2013)) than are presented here. Overall, because DLS measurements allow for multi-modal fitting models, we considered them to be a better way to measure Rh values for the wild-type and stabilized SOSIP.664 trimers.

Small angle X-ray scattering (SAXS)

SAXS measurements were conducted on Beam Line 4-2 at the Stanford Synchrotron Radiation Laboratory (Smolsky et al., 2007). The focused 11 keV X-ray beam irradiated a thin-wall quartz capillary cell, placed 2.5 m upstream of the Rayonix MX 225HE detector (Evanston, IL). A 50 µl sample of various PGT145-

purified BG505 SOSIP.664 trimer variants (1 – 2 mg/ml) were injected onto a high resolution Sepharose-200 column (GE Healthcare) with a flow rate of 50 µl/min in 20 mM Na_3PO_4 pH 7.4, 150 mM NaCl, 0.02 % NaN_3, 1 mM EDTA. The column eluate passed through a UV detector cell and into the quartz capillary cell. X-ray exposures were collected for 1 s every 5 s throughout the run, during which a circulating water bath maintained the capillary cell temperature at 8°C. The detector pixel numbers were converted to the momentum transfer using the formula: q = 4p*sinq/l, where l is the X-ray wavelength of 1.127 Å and 2*q is the scattering angle calibrated using a silver behenate powder standard placed at the capillary position. A background scattering curve was obtained from the first 100 exposures (before the void volume), and was subtracted from all subsequent exposures during generation of the sample elution profile. The radius of gyration values (R_g) and I(0) for each frame were batch-analyzed using AutoRg, and frames with stable R_g values were merged using Primus (Petoukhov et al., 2007) for the final scattering curve . The real space distance distribution functions were calculated from the merged data sets by indirect transformation using the program GNOM (Svergun, 1992).

Hydrogen-deuterium exchange coupled with mass spectrometry (HDX-MS)

Two domain soluble CD4 (sCD4) (Garlick et al., 1990) was obtained from the NIH AIDS Reagents Repository. Immediately before HDX-MS analysis, all proteins were SEC-purified using a Superdex S200 column (GE Healthcare) and a PBS-based elution buffer (20 mM sodium phosphate pH 7.4, 150 mM NaCl with 1 mM EDTA and 0.02 % sodium azide). Complexes were formed by overnight incubation at 4°C with a 9-fold molar excess of sCD4 (relative to one trimer). Native gels were run for each sample to assess complex formation (SI Fig. 4C). Various PGT145-purified BG505 SOSIP.664 trimers (15 µg) were diluted 10-fold into deuterated PBS buffer and incubated at room temperature. The deuterium exchange reactions were quenched after 3 s, 1 min, 30 min and 20 h by mixing with an equal volume of cold 200 mM Tris-(2-Carboxyethyl)phosphine hydrochloride (TCEP), 0.2 % formic acid (final pH 2.5). The samples were subsequently digested with pepsin (0.15 mg/ml) for 5 min on ice, flash frozen in liquid nitrogen, stored at -80°C and analyzed by LC-MS as

described previously (Guttman et al., 2014). Differences in exchange profiles that exceeded the error, based on the standard deviation from duplicate measurements, were visualized on the trimer structure using custom macros in PyMOL (Schrodinger LLC, 2010).

Negative-stain electron microscopy (EM)

Purified BG505, B41, ZM197M and AMC008 SOSIP.664 trimers, either alone or as Fab complexes (with PGV04 and 35O22), were analyzed by negative-stain EM. To form complexes, a 6-10 molar excess of each Fab was incubated with trimers overnight at room temperature. A 3 µl aliquot containing ~0.03 mg/ml of a trimer or Fab-trimer complex was applied for 5 s onto a carbon-coated 400 Cu mesh grid that had been glow discharged at 20 mA for 30 s, then negatively stained with 2% (w/v) uranyl formate for 60 s. Data were collected on either an FEI Tecnai T12 electron microscope operating at 120 keV, with an electron dose of ~25 $e^-/Å^2$ and a magnification of 52,000x that resulted in a pixel size of 2.05Å at the specimen plane, or an FEI Talos electron microscope operating at 200 keV, with an electron dose of ~25 $e^-/Å^2$ and a magnification of 92,000x that resulted in a pixel size of 1.57 Å at the specimen plane. Images were acquired with a Tietz TemCam-F416 CMOS camera (FEI Tecnai T12) or FEI Ceta 16M camera (FEI Talos) using a nominal defocus range of 1000-1500 nm.

Image processing and 3D reconstruction

Data processing methods are described in detail elsewhere, including the closed, partially open, and non-native trimer classification system (Derking et al. 2015; Pugach et al. 2015). Briefly, a total of 24,522 particles were included in the final reconstruction for the 3D average of AMC008 SOSIP.v4.2 in complex with PGV04 and 35O22 Fabs. An initial common-lines model was generated using 2D class averages in EMAN2 (Tang et al., 2007) followed by refinement against all particles in Sparx (Penczek et al., 1994). The resolution of the final reconstruction is ~15 Å based on a Fourier shell correlation of 0.5 (Fig. S5A-C).

Isothermal titration calorimetry (ITC)

ITC was performed using an Auto-iTC 200 instrument (GE Healthcare) using a protocol similar to one described previously (Julien et al., 2013; Sanders et al., 2013). Briefly, prior to conducting the titrations, proteins were dialyzed against Tris-saline buffer (150 mM NaCl, 20 mM Tris, pH 8.0). Absorbance at 280 nm using calculated extinction coefficients was used to determine and adjust protein concentrations. The ligand present in the syringe was 19b IgG at a concentration of 10-20 μM, while BG505, B41 or AMC008 SOSIP.664 trimers were present in the cell at a concentration of 4-6 μM. In each binding experiment, a 5 μcal reference power determination preceded the first injection of 0.5 μl, which was followed by 15 injections of 2.5 μl each at intervals of 180 s. Origin 7.0 software was used to derive the affinity constants (K_D), the molar reaction enthalpy (ΔH), and the stoichiometry of binding (N), by fitting the integrated titration peaks via a single-site model or a two-site model, as appropriate.

Glycan profiling

Env trimers (10 μg) were resolved by SDS-PAGE under non-reducing conditions, followed by staining with Coomassie Blue. Bands corresponding to gp140 were excised from the gels and washed alternately with acetonitrile and water, five times. N-linked glycans were then released by addition of protein N-glycosidase F (PNGase F) at 5000 U/ml and incubation at 37°C for 16 h, according to the manufacturer's instructions (New England Biolabs). The released glycans were subsequently eluted from gel bands by extensive washing with water, and then dried using a SpeedVac concentrator. Released glycans were labelled with 2-aminobenzoic acid (2-AA) as previously described (Neville et al., 2009). Briefly, glycans were resuspended in 30 μl of water followed by addition of 80 μl of labelling mixture (comprising 30 mg/ml 2-AA and 45 mg/ml sodium cyanoborohydride in a solution of sodium acetate trihydrate [4% w/v] and boric acid [2% w/v] in methanol). Samples were then incubated at 80°C for 1 h. Excess label was removed using Spe-ed Amide-2 cartridges, as previously described (Neville et al., 2009). Fluorescently labelled glycans were resolved by hydrophilic interaction liquid

chromatography-ultra performance liquid chromatography (HILIC-UPLC) using a 2.1 mm × 10 mm Acquity BEH Amide Column (1.7 μm particle size) (Waters). The following gradient was run: time = 0 min (t = 0): 22.0% A, 78.0% B (flow rate of 0.5 ml/min); t = 38.5: 44.1% A, 55.9% B (0.5 ml/min); t = 39.5: 100% A, 0% B (0.25 ml/min); t = 44.5: 100% A, 0% B (0.25 ml/min); t = 46.5: 22.0% A, 78.0% B (0.5 ml/min), t = 48: 22.0% A, 78.0% B (0.5 ml/min), where solvent A was 50 mM ammonium formate, pH 4.4, and solvent B was acetonitrile. Fluorescence was measured using an excitation wavelength of 250 nm and a detection wavelength of 428 nm. Data processing was performed using Empower 3 software.

The percentage abundance of oligomannose-type glycans was calculated by integration of the relevant peak areas before and after Endoglycosidase H digestion, following normalization. Digestions were performed on free glycans at 37°C for 16 h. The digested glycans were purified using a polyvinylidene fluoride (PVDF) protein-binding membrane plate (Millipore) prior to HILIC-UPLC analysis.

Immunizations

Groups of 6-week old Balb/cJ or 129S1/SvlmJ mice were immunized as described (Hu et al., 2015) with 10 μg of BG505 SOSIP.664 or SOSIP.v4.1 trimers in 0.2-0.4 μg ISCOMATRIX™ adjuvant (CSL Ltd) via footpad injections. The first immunization (week 0) was followed by booster immunizations at weeks 4 and 16. For the final immunization (week 16), the mice were given 20 μg of trimer in ISCOMATRIX™, and they were then bled at week 18.

Rabbits (5 per group) were immunized as described with 22 μg of PGT145-purified trimers at week 0, 4 and 20, and NAb responses were assessed at week 22 (Sanders et al., 2015). The rabbit sera were assayed for autologous and cross-reactive NAbs using Env-pseudoviruses in the TZM-bl cell assay (Montefiori, 2009), and for trimer-binding antibodies by D7324-capture ELISA (Sanders et al., 2013). The Env-pseudotyped viruses and their Tier classifications have been described elsewhere (deCamp et al., 2014; Goo et al., 2014; Li et al., 2006; Seaman et al., 2010; Simek et al., 2009). When the neutralization-sensitivity of the parental AMC008 virus was assessed using a panel of human sera and MAbs and a panel of test viruses

at the Duke University Medical Center, it was classified as being in Tier-1B (not shown), while the BG505.T332N virus has a Tier-2 phenotype (Sanders et al., 2015). Note that the autologous AMC008 and BG505.T332N viruses do not contain the stabilizing mutations described in this manuscript.

Supplemental figure legends

Figure S1. Screening of stabilizing mutations using unpurified AMC008, BG505, B41 and ZM197M SOSIP.664 proteins, related to figure 1. BN-PAGE analysis of unpurified (**A**) AMC008, (**B**) BG505, (**C**) B41 SOSIP.664 variants, followed by Western blotting with 2G12. In the AMC008 SOSIP.664 context, the A316W, I535M and L543N substitutions make a substantial contribution to trimer formation, both individually and collectively. We note that introducing the reverse N543L substitution into BG505 SOSIP.664 reduced trimer formation (data not shown). (**D**) Use of a novel thermostability assay to screen unpurified BG505 SOSIP.664-D7324 variants. Culture supernatants from 293T cells were incubated for 30 min at temperatures ranging from 39–77°C, then analyzed by D7324-capture ELISA with 2G12 detection. The binding of 2G12 is plotted as a function of temperature, with the OD_{450} value at 39°C set at 100%. The A316W substitution increases thermostability. (**E**) The unfolding pattern of the variant proteins was visualized by plotting the first derivative of the graph in (**D**) using GraphPad prism 5. (**F**) The T_m values were derived from the peaks in the first derivative curves shown in (**D**). The T_m values obtained in this assay are highly reproducible (standard deviation of ± 0.3°C for BG505 SOSIP.664-D7324). (**G**) Correlation plot between T_m values obtained using unpurified BG505 SOSIP.664-D7324 proteins in the above thermostability assay and T_m values obtained using PGT145-purified BG505 SOSIP.664-D7324 trimers in a DSC assay (Table 1; Fig. S2E). (**H**) Competition ELISA using wild-type and A316W-substituted BG505-V3 peptides. Increasing concentrations of wild-type (light green) or A316W-substituted (dark green) peptides were incubated with the V3 non-NAb 39F (1.0 μg/ml) prior to addition to immobilized, PGT145-purified BG505 SOSIP.664-D7324 trimers. As the two

peptides were equally effective at binding 39F and impeding its binding to the trimers, the A316W substitution does not directly affect the 39F epitope. Similar results were obtained with two other V3 non-NAbs, 19b and 14e (data not shown). (**I**) High-throughput mutagenesis screen at position 316 of BG505 SOSIP.664-D7324, with a capture ELISA endpoint. Wild-type or position 316-mutated variant Env proteins in culture supernatants from transiently transfected 293T cells were captured via D7324. The bound proteins were detected using either PGT145 (0.11 μg/ml; to detect native trimers) or 14e (0.5 μg/ml; to detect V3 exposure), and the ratios of the OD_{450} signals were plotted. The wild-type residue (alanine) is shown in grey, the designed mutant (tryptophan) in red and other substituted amino acids in black. Only bulky hydrophobic amino acids reduce V3 non-NAb binding. (**J, K**) Spontaneous sampling of the CD4i conformation was assessed using a D7324-capture ELISA. CD4i epitope exposure was assessed by measuring the binding of high concentrations (10 μg/ml) of non-NAbs (**J**) 17b and (**K**) 412d. The OD_{450} values obtained using the wild-type BG505 SOSIP.664-D7324 protein were set at 100% and used to normalize the values for the E64K and H66R mutants. Mock indicates blank transfection supernatant.

Figure S2. The effect of stabilizing mutations on the biochemical and biophysical properties of AMC008, BG505, B41 and ZM197M SOSIP.664 proteins, related to table 1. (**A**) The PGT145-purified SOSIP.664 proteins were analyzed by BN-PAGE analysis and found to be exclusively trimeric. (**B**) Reducing (+DTT) and non-reducing (-DTT) SDS-PAGE analysis of the same proteins. The complete conversion of gp140 bands into gp120 when DTT is present indicates gp120-gp41 cleavage is efficient; there are also no indications that the purified trimers form higher m.wt. disulfide-linked oligomers. (**C**) Negative-stain EM analyses of 2G12/SEC-purified (top left panel) or PGT145-purified (all other panels) AMC008, BG505, B41 and ZM197M SOSIP.664 trimer variants. The 2D class averages are shown. Based on loop-movement, compactness and angles between individual protomers, the trimers are classified as closed native-like, partially open native-like or non-native (Pugach et al., 2015). Native-like trimers are regularly

shaped and have the highest concentration of electron density at the particle center (usually shaped like a triangle because Env is trimeric). The absence or presence of additional density around this center of mass determines whether trimers are classified as closed native-like or partially open native-like, respectively. Non-native forms are often elongated and no triangular center of density is visible. The classifications are quantified below each panel. The percentages of closed and partially open native-like trimers are in green, and of non-native forms in red. The total number of particles classified is defined as 100%. We observe +/-5% variation between experiments.

Figure S3. The effect of stabilizing mutations on the biochemical and biophysical properties of AMC008, BG505, B41 and ZM197M SOSIP.664 proteins, related to table 1. (**A**) SEC profiles of 2G12- or PGT145-purified BG505 SOSIP.664 and SOSIP.v4.1 trimers. (**B**) DSC analysis of PGT145-purified AMC008, BG505, B41 and ZM197M SOSIP.664 trimer variants. The unfolding patterns were fitted using a non-two state model, revealing three individual unfolding peaks. The T_m values of the individual peaks are listed in Table S1. For simplification, the data were also fitted to a two-state model and the T_m values of those analyses are provided in Table 1. (**C**) SAXS analysis of PGT145-purified BG505 SOSIP.664 and SOSIP.v4 trimers. The merged SAXS data are shown for the BG505 trimers (upper panel). Lower panel: summary of SAXS and DLS derived structural parameters. The radii of gyration (R_g) were derived from SAXS experiments using both Guinier analysis with a q*Rg range of 1 - 1.3, and from the particle distance distribution plots obtained from indirect transformation using GNOM (Svergun, 1992). The standard deviations of the R_h and R_g values were small, and similar between the different constructs (+/- 0.2-0.5 Å). (**D**) Glycan profiles of PGT145-purified SOSIP.664 variants as determined by HILIC-UPLC. The percentages of $Man_{5-9}GlcNAc_2$ glycans (M5-M9), as a proportion of the total glycan population, are listed in Table 1

Figure S4. The effect of stabilizing mutations on HDX profiles of BG505 SOSIP.664 trimers, related to figure 2. (**A, B**) Left panels: Butterfly plots of HDX profiles in the absence of CD4. (**A**) PGT145-purified BG505 SOSIP.664 *vs.* SOSIP.v4.1 trimers; (**B**) PGT145-purified BG505 SOSIP.664 *vs.* SOSIP.v4.2 trimers. Right panels: The differences in exchange patterns are mapped onto the higher resolution BG505 SOSIP.664 structure (Pancera et al., 2014). Regions that are less or more protected from deuterium exchange are colored red and blue, respectively. The positions of the stabilizing mutations are indicated in green. (**C**) BN-PAGE gel-shift analysis of BG505 SOSIP.664 wild-type and double mutant trimers in the presence of sCD4 (0.55 mg/ml; i.e., in 9-molar excess per trimer. For all three trimers, there is a complete band-shift in the presence of sCD4, which shows that saturating binding of CD4 occurs in each case. However, note that the wild-type trimers dimerize when CD4 binds, but the two double mutants do not. The large conformational changes upon CD4 binding in the wild-type protein might result in dimerization via the flexible variable loops, which is not the case for the mutants, as conformational changes are largely prevented upon CD4 binding.

Figure S5. Negative-Stain EM of PGV04 and 35O22 Fabs bound to AMC008 SOSIP.v4.2, related to figure 3. (A) 2D class averages and **(B)** 2D projections of the 3D model. **(C)** Fourier shell correlation (FSC) curve of the refined map. The resolution of the final map calculated from the FSC function at 0.5 is 15 Å.

Figure S6: Ab responses in SOSIP.664 or SOSIPv4.1 immunized mice and rabbits, related to figure 4. (**A**) Ab responses to BG505 SOSIP.664 trimers were quantified in mouse sera drawn at week-18 by D7324-capture ELISA, using BG505 SOSIP.664-D7324. The mice were immunized with PGT145-purified BG505 SOSIPv4.1 or BG505 SOSIP.664 trimers at weeks 0, 4, and 16. Midpoint binding Ab titers in rabbit sera were also measured by D7324-capture ELISA, using (**B**) SOSIP.664-D7324 or (**C**) SOSIP.v4-D7324 trimers as the test antigen. Rabbits were immunized at week 0, 4 and 20 and the Ab responses were analyzed at week 22. Blue symbols represent BG505 trimer-immunized animals, red symbols AMC008.

The SOSIP.664 recipients are shown by closed circles, SOSIP.v4 by squares. (**D**) The ratios of the SOSIP.664/SOSIP.v4 midpoint titers are plotted. (**E**) As an alternative to direct V3-peptide ELISA, the V3 Ab response was also determined by pre-incubating the sera with a cyclized V3 peptide before determining the residual anti-trimer binding titers by ELISA (see methods). The relative V3 Ab responses (as a % of the total anti-trimer Ab responses) were calculated by comparing the midpoint titers in the absence and presence of the V3 peptide. Correlation plots between autologous BG505 NAb titers and either (**F**) BG505 SOSIP.664 binding Ab titers, or (**G**) BG505 SOSIP.v4 binding Ab titers. The correlation was slightly stronger when the NAb titer comparison was with SOSIP.v4-D7324 binding Ab titers. Correlation plots between autologous AMC008 NAb titers and either (**H**) AMC008 SOSIP.664 binding Ab titers, or (**I**) AMC008 SOSIP.v4 binding Ab titers. The strong correlation with the binding Ab titers to the AMC008 SOSIP.v4-D7324 trimers implies that AMC008 SOSIP.v4 trimers present neutralization-relevant epitopes *in vivo* more efficiently than their SOSIP.664 counterparts. The r and p values for non-parametric Spearman correlations are shown. Statistical comparisons between groups were performed using a two-tailed Mann-Whitney U test (*p>0.05, **p>0.01, ***p>0.001).

Data S1: Supportive data for ELISA and HDX experiments, related to figure 3 and table 2. (**A-D**) ELISA binding curves for bNAbs and non-NAbs to unpurified SOSIP.664 wild-type and mutant proteins based on the following genotypes: (**A**) AMC008; (**B**) BG505; (**C**) B41; (**D**) ZM197M. (**E-H**) ELISA binding curves for bNAbs and non-NAbs to PGT145 purified SOSIP.664 wild-type and mutant proteins based on the following genotypes (**E)** AMC008; (**F**) BG505; (**G**) B41; (**H**) ZM197M SOSIP.664-D7324 trimer variants. (**I**) Exchange profiles for all the individual peptides. The percentage of deuterium exchange at each time point (3 s, 1 min, 30 min, 20 h) is shown for the three trimers ± CD4.

Tables

Table S1: Detailed DSC analysis of PGT145-purified SOSIP trimer variants, related to table 1. In addition to the simplified two-state model analysis, the unfolding patterns were fitted using a non-two state model (see Fig. S3B), revealing three individual unfolding peaks. The T_m values of the individual peaks are given in °C.

		DSC				
	Stabilizing mutations	**Two state model**	**Independent non-two state model**			
AMC008	**SOSIP.664 (2G12-SEC)**	59.6				
	SOSIP.664 (PGT145)	60.2	56.1	57.9	60.6	
	v3.2	61.6	58.5	60.5	62.6	
	v4.1	64.5	63.3	64.1	65.3	
	v4.2	64.0	62.4	63.3	64.6	
BG505	**SOSIP.664 (2G12-SEC)**	67.3				
	SOSIP.664 (PGT145)	66.7	64.4	65.8	67.4	
	E64K	67.9	64.2	66.3	68.3	
	H66R	67.5	65.9	67.4	68.4	
	A316W	69.0	66.9	68.3	69.7	
	v4.1	69.5	66.6	68.3	70.2	
	v4.2	69.3	66.6	68	70.0	
B41	**SOSIP.664 (2G12-SEC)**	57.6				
	SOSIP.664 (PGT145)	58.6	55.3	57.5	59	
	v4.1	61.7	58.9	60.3	62.3	
	v4.2					
ZM197M	**SOSIP.664 (2G12-SEC)**					
	SOSIP.664 (PGT145)	62.2	58.6	60.8	62.9	76.3
	v4.1					
	v4.2	62.6		62.2	63.6	76.1

Table S2. Amino acids present at positions 535 and 543 of the α6 helix in gp41, related to figure 1. The amino acids present in the wild-type sequences of clones JR-FL, KNH1144, BG505, B41, ZM197M and AMC008 at positions 535 and 543, as well as the amino acids optimal for Env stability (in green; (Dey et al., 2008; Leaman and Zwick, 2013)) are shown. The right-most column specifies the amino acid changes that have now been incorporated into the various SOSIP.664 constructs to optimize trimer formation (resulting in the SOSIP.v3 trimers).

Subtype	Envelope	Residue 535	Residue 543	Amino-acid change
B	JRFL	M	L	
A	KNH144	I	Q	
A	BG505	M	N	No change
	Optimal	**M**	**N / Q**	
B	B41	M	L	L543N
B	AMC008	I	L	I535M + L543N
C	ZM197M	V	Q	V535M

Table S3. Nomenclature for new stabilized SOSIP.664 trimers, related to figure 1. An overview of the modifications made to the stabilized SOSIP.664 trimer variants. Green, present; red, not present. SOSIP.681 and SOSIP.664 were renamed to SOSIP.v1 and SOSIP.v2 respectively. R6 refers to an improved hexa-arginine furin cleavage site (Binley et al., 2002).

			A501C-T605C	I559P	R6	ΔMPER	I535M	L543Q	L543N	A316W	E64K	H66R
SOSIP.681	SOSIP.v1	SOSIP.v1										
SOSIP.664	SOSIP.v2	SOSIP.v2										
	SOSIP.v3	SOSIP.v3.1										
		SOSIP.v3.2										
	SOSIP.v4	SOSIP.v4.1										
		SOSIP.v4.2										

Table S4. Midpoint neutralization titers for sera from rabbits immunized with SOSIP.664 or SOSIP.v4 trimers tested against a panel of Env-pseudotyped viruses, related to figure 4. The TZM-bl cell assay was performed at AMC. ID_{50} values, i.e., the week-22 serum dilution at which infectivity was inhibited by 50%, are recorded, with the boxes colored according to their magnitude. White, no neutralization, ID_{50} <40; yellow, weak neutralization, ID_{50} 40-100; orange, moderate neutralization, ID_{50} 100-1000; red, strong neutralization, ID_{50} >1000. Values in columns labeled with "V3 pep" were obtained in the presence of V3 peptide as competitor (Sanders et al., 2015).

	virus	BG 505	BG 505	AMC 008	AMC 008	B41	SF162	SF162	BaL	92UG	WITO	REJO	92RW	AC10	SHIV p3	MLV
	Tier	2	2	1B	1B	2	1A	1A	1B	2	2	2	2	2	2	Neg Ctrl
	Clade	A	A	B	B	B	B	B	B	A	B	B	A	B	B	
Immunogen	**Rabbit ID**		**V3 pep**		**V3 pep**			**V3 pep**								
BG505 SOSIP.664	1569	116	157	29	22	ND	339	<20	41	<20	<20	22	28	<20	<20	<20
	1570	10013	>4860	27	<20	ND	137	<20	30	<20	<20	<20	20	<20	<20	<20
	1571	71	54	67	28	ND	253	23	39	<20	<20	<20	33	<20	26	<20
	1572	10925	>4860	55	27	ND	50	38	41	22	<20	<20	23	<20	<20	<20
	1573	8110	>4860	<20	<20	ND	132	<20	93	<20	<20	<20	<20	<20	<20	<20
BG505 SOSIP.v4.1	1574	23931	>4860	24	28	ND	292	23	92	42	<20	89	69	<20	<20	<20
	1575	4521	>4860	<20	<20	ND	<20	<20	<20	<20	<20	<20	<20	<20	26	21
	1576	577	608	25	22	ND	60	<20	21	<20	<20	<20	<20	20	23	<20
	1577	4352	>4860	<20	<20	ND	24	24	<20	<20	<20	<20	21	<20	38	<20
	1578	4485	>4860	50	39	ND	130	21	49	<20	43	21	25	20	48	<20
BG505 SOSIP.v4.2	1579	5353	>4860	<20	23	ND	21	<20	<20	<20	21	<20	33	25	35	<20
	1580	4963	>4860	<20	<20	ND	175	<20	<20	<20	32	<20	24	<20	32	<20
	1581	4048	>4860	<20	<20	ND	<20	<20	<20	<20	22	<20	33	<20	<20	<20
	1582	4561	>4860	<20	20	ND	<20	<20	<20	<20	42	<20	24	<20	<20	<20
	1583	987	2008	<20	<20	ND	<20	<20	<20	<20	<20	<20	24	<20	<20	<20
AMC008 SOSIP.664	1594	<20	<20	99	102	ND	823	132	122	<20	27	29	<20	<20	32	<20
	1595	<20	<20	276	312	ND	1217	810	319	<20	23	32	25	<20	41	<20
	1596	<20	<20	210	153	ND	4028	75	262	<20	<20	24	25	20	43	<20
	1597	<20	<20	360	197	ND	208	94	315	<20	28	<20	<20	<20	28	<20
	1598	<20	<20	260	159	ND	423	68	138	<20	<20	22	<20	<20	<20	<20
AMC008 SOSIP.v4.1	1599	<20	<20	705	608	ND	1227	220	2134	<20	<20	<20	<20	<20	68	<20
	1600	<20	<20	241	63	ND	3344	32	261	<20	<20	21	<20	<20	40	<20
	1601	<20	<20	269	95	ND	3620	90	157	<20	<20	37	27	27	43	<20
	1602	<20	<20	380	258	ND	919	240	202	<20	<20	28	<20	<20	47	<20
	1603	<20	<20	106	30	ND	48	29	24	<20	<20	<20	<20	<20	32	<20
AMC008 SOSIP.v4.2	1604	<20	<20	219	77	ND	117	67	35	<20	<20	<20	<20	23	65	<20
	1605	<20	<20	299	95	ND	131	41	43	<20	27	<20	<20	<20	100	<20
	1606	<20	<20	262	138	ND	298	54	71	<20	41	20	<20	21	76	<20
	1607	<20	<20	272	118	ND	1080	42	78	<20	48	<20	29	<20	49	<20
	1608	<20	<20	178	82	ND	315	63	70	<20	27	<20	25	<20	66	<20
B41 SOSIP.664	1639	<20	ND	94	ND	1484	2820	ND	368	<20	<20	<20	ND	ND	<20	<20
	1640	<20	ND	58	ND	1179	2730	ND	186	28	21	42	ND	ND	42	<20
	1641	<20	ND	41	ND	149	230	ND	97	24	26	39	ND	ND	39	<20
	1642	<20	ND	128	ND	838	5989	ND	293	<20	20	37	ND	ND	37	<20
	1643	<20	ND	216	ND	44	2026	ND	507	<20	<20	32	ND	ND	32	<20
B41 SOSIP.v4.1	1644	<20	ND	<20	ND	<20	263	ND	34	<20	<20	21	ND	ND	21	<20
	1645	<20	ND	<20	ND	1560	128	ND	<20	<20	<20	<20	ND	ND	<20	<20
	1646	<20	ND	26	ND	1048	376	ND	96	<20	<20	28	ND	ND	28	<20
	1647	<20	ND	<20	ND	795	88	ND	32	<20	<20	25	ND	ND	25	<20
	1648	<20	ND	<20	ND	1446	495	ND	80	<20	<20	<20	ND	ND	<20	<20

Table S5. Midpoint neutralization titers for sera from immunized rabbits with SOSIP.664 or SOSIP.v4 trimers and tested against a panel of Env-pseudotyped viruses, related to figure 4. The TZM-bl cell assay was performed at DUMC. ID_{50} values, i.e., the week-22 serum dilution at which infectivity was inhibited by 50%, are recorded, with the boxes colored according to their magnitude. White, no neutralization, ID_{50} <40; yellow, weak neutralization, ID_{50} 40-100; orange, moderate neutralization, ID_{50} 100-1000; red, strong neutralization, ID_{50} >1000.

	virus	BG505	AMC008	B41	MN.3	SF162	MW965.26	257102.43	TRO.11	BJOX002000.03.2	X1632-S2-B10	Ce1176_A3	246-F3_C10_2	CH119.10	Ce703010217_B6	CNE55	MLV
	Tier Clade	2 A	1B B	2 B	1A B	1A B	1A C	2 C	2 B	2 BC	2 B	2 C	2 AC	2 BC	2 A	2 AE	Neg Ctrl
Immunogen	**Rabbit ID**																
BG505 SOSIP.664	1569	27	<20	ND	266	392	ND	<20	<20	<20	<20	<20	<20	<20	<20	<20	<20
	1570	2368	<20	ND	141	286	ND	<20	<20	<20	<20	<20	<20	<20	<20	<20	<20
	1571	<20	<20	ND	475	276	ND	<20	<20	<20	<20	<20	<20	<20	<20	<20	<20
	1572	2274	<20	ND	36	580	ND	<20	<20	<20	<20	<20	<20	<20	<20	<20	<20
	1573	3654	<20	ND	523	265	ND	<20	<20	<20	<20	<20	<20	<20	<20	<20	<20
BG505 SOSIP.v4.1	1574	11626	<20	ND	6130	391	ND	<20	<20	<20	<20	<20	<20	<20	<20	<20	<20
	1575	837	<20	ND	<20	<20	ND	<20	<20	<20	<20	<20	<20	<20	<20	<20	<20
	1576	50	<20	ND	80	<20	ND	<20	<20	<20	<20	<20	<20	<20	<20	<20	<20
	1577	2659	<20	ND	<20	<20	ND	<20	<20	<20	<20	<20	<20	<20	<20	<20	<20
	1578	6270	<20	ND	396	277	ND	<20	<20	<20	<20	<20	<20	<20	<20	<20	<20
BG505 SOSIP.v4.2	1579	1190	<20	ND	27	<20	ND	<20	<20	<20	<20	<20	<20	<20	<20	<20	<20
	1580	2022	<20	ND	<20	44	ND	<20	<20	<20	<20	<20	<20	<20	<20	<20	<20
	1581	627	<20	ND	<20	32	ND	<20	<20	<20	<20	<20	<20	<20	<20	<20	<20
	1582	1556	<20	ND	<20	<20	ND	<20	<20	<20	<20	<20	<20	<20	<20	<20	<20
	1583	738	<20	ND	46	<20	ND	<20	<20	<20	<20	<20	<20	<20	<20	<20	<20
AMC008 SOSIP.664	1594	<20	<20	ND	1183	1892	ND	<20	<20	<20	<20	<20	<20	<20	<20	<20	<20
	1595	<20	186	ND	1111	5235	ND	<20	<20	<20	<20	<20	<20	<20	<20	<20	<20
	1596	<20	46	ND	7117	5249	ND	<20	<20	<20	<20	<20	<20	<20	<20	<20	<20
	1597	<20	242	ND	427	337	ND	<20	<20	<20	<20	<20	<20	<20	<20	<20	<20
	1598	<20	29	ND	3668	899	ND	<20	<20	<20	<20	<20	<20	<20	<20	<20	<20
AMC008 SOSIP.v4.1	1599	<20	706	ND	2173	593	ND	<20	<20	<20	<20	<20	<20	<20	<20	<20	<20
	1600	<20	83	ND	3285	2364	ND	<20	<20	<20	<20	<20	<20	<20	<20	<20	<20
	1601	<20	169	ND	5782	1466	ND	<20	<20	<20	<20	<20	<20	<20	<20	<20	<20
	1602	<20	363	ND	1342	481	ND	<20	<20	<20	<20	<20	<20	<20	<20	<20	<20
	1603	<20	<20	ND	104	<20	ND	<20	<20	<20	<20	<20	<20	<20	<20	<20	<20
AMC008 SOSIP.v4.2	1604	<20	<20	ND	287	154	ND	<20	<20	<20	<20	<20	<20	<20	<20	<20	<20
	1605	<20	49	ND	713	54	ND	<20	<20	<20	<20	<20	<20	<20	<20	<20	<20
	1606	<20	87	ND	829	210	ND	<20	<20	<20	<20	<20	<20	<20	<20	<20	<20
	1607	<20	62	ND	2598	326	ND	<20	<20	<20	<20	<20	<20	<20	<20	<20	<20
	1608	<20	115	ND	2464	200	ND	<20	<20	<20	<20	<20	<20	<20	<20	<20	<20
B41 SOSIP.664	1639	<20	<20	249	2443	ND	554	<20	<20	<20	<20	28	<20	<20	<20	<20	<20
	1640	<20	<20	965	818	ND	847	<20	<20	<20	<20	<20	<20	<20	<20	<20	<20
	1641	<20	<20	111	333	ND	134	<20	<20	<20	<20	24	<20	25	<20	26	<20
	1642	<20	22	601	1733	ND	387	<20	<20	<20	<20	<20	<20	<20	<20	<20	<20
	1643	<20	24	<20	4127	ND	2406	<20	<20	<20	<20	<20	<20	<20	<20	<20	<20
B41 SOSIP.v4.1	1644	<20	<20	<20	155	ND	179	<20	<20	<20	<20	<20	<20	<20	<20	<20	<20
	1645	<20	<20	390	156	ND	71	<20	<20	<20	<20	<20	<20	<20	<20	<20	<20
	1646	<20	<20	640	554	ND	157	<20	<20	<20	<20	21	<20	27	22	<20	<20
	1647	<20	<20	206	214	ND	191	<20	<20	<20	<20	<20	<20	<20	<20	<20	<20
	1648	<20	<20	1122	943	ND	192	<20	<20	<20	<20	<20	<20	35	<20	<20	<20

References

Binley, J.M., Sanders, R.W., Clas, B., Schuelke, N., Master, A., Guo, Y., Kajumo, F., Anselma, D.J., Maddon, P.J., Olson, W.C., et al. (2000). A recombinant human immunodeficiency virus type 1 envelope glycoprotein complex stabilized by an intermolecular disulfide bond between the gp120 and gp41 subunits is an antigenic mimic of the trimeric virion-associated structure. J. Virol. *74*, 627–643.

Binley, J.M., Sanders, R.W., Master, A., Cayanan, C.S., Wiley, C.L., Schiffner, L., Travis, B., Kuhmann, S., Burton, D.R., Hu, S., et al. (2002). Enhancing the proteolytic maturation of human immunodeficiency virus type 1 envelope glycoproteins. J. Virol. *76*, 2606–2616.

Derking, R., Ozorowski, G., Sliepen, K., Yasmeen, A., Cupo, A., Torres, J.L., Julien, J., Lee, J.H., van Montfort, T., de Taeye, S.W., et al. (2015). Comprehensive antigenic map of a cleaved soluble HIV-1 envelope trimer. PLoS Pathog. *11*, e1004767.

Dey, A.K., David, K.B., Ray, N., Ketas, T.J., Klasse, P.J., Doms, R.W., and Moore, J.P. (2008). N-terminal substitutions in HIV-1 gp41 reduce the expression of non-trimeric envelope glycoproteins on the virus. Virology *372*, 187–200.

Euler, Z., van Gils, M.J., Bunnik, E.M., Phung, P., Schweighardt, B., Wrin, T., and Schuitemaker, H. (2010). Cross-reactive neutralizing humoral immunity does not protect from HIV type 1 disease progression. J. Infect. Dis. *201*, 1045–1053.

Garlick, R.L., Kirschner, R.J., Eckenrode, F.M., Tarpley, W.G., and Tomich, C.S. (1990). Escherichia coli expression, purification, and biological activity of a truncated soluble CD4. AIDS Res. Hum. Retroviruses *6*, 465–479.

Guttman, M., Garcia, N.K., Cupo, A., Matsui, T., Julien, J.P., Sanders, R.W., Wilson, I.A., Moore, J.P., and Lee, K.K. (2014). CD4-induced activation in a soluble HIV-1 Env trimer. Structure *22*, 974–984.

Julien, J.-P., Lee, J.H., Cupo, A., Murin, C.D., Derking, R., Hoffenberg, S., Caulfield, M.J., King, C.R., Marozsan, A.J., Klasse, P.J., et al. (2013). Asymmetric recognition of the HIV-1 trimer by broadly neutralizing antibody PG9. Proc. Natl. Acad. Sci. U. S. A. *110*, 4351–4356.

Julien, J.-P., Lee, J.H., Ozorowski, G., Hua, Y., Torrents de la Peña, A., de Taeye, S.W., Nieusma, T., Cupo, A., Yasmeen, A., Golabek, M., et al. (2015). Design and structure of two HIV-1 clade C SOSIP.664 trimers that increase the arsenal of native-like Env immunogens. Proc. Natl. Acad. Sci. U. S. A. *112*, 11947–11952.

Kirschner, M., Monrose, V., Paluch, M., Techodamrongsin, N., Rethwilm, A., and Moore, J.P. (2006). The production of cleaved, trimeric human immunodeficiency virus type 1 (HIV-1) envelope glycoprotein vaccine antigens and infectious pseudoviruses using linear polyethylenimine as a transfection reagent. Protein Expr. Purif. *48*, 61–68.

Klasse, P.J., Cupo, A., Cocco, N., Korzun, J., Yasmeen, A., Ward, A.B., Wilson, I.A., Sanders, R.W., and Moore, J.P. (2013). Influences on trimerization and aggregation of soluble , cleaved HIV-1 SOSIP envelope glycoprotein. J. Virol. *87*, 9873–9885.

Leaman, D.P., and Zwick, M.B. (2013). Increased functional stability and homogeneity of viral envelope spikes through directed evolution. PLoS Pathog. *9*, e1003184.

Montefiori, D.C. (2009). Measuring HIV neutralization in a luciferase reporter gene assay. Methods Mol. Biol. *485*, 395–405.

Neville, D.C.A., Dwek, R.A., and Butters, T.D. (2009). Development of a single column method for the separation of lipid- and protein-derived oligosaccharides. J. Proteome Res. *8*, 681–687.

Pancera, M., Zhou, T., Druz, A., Georgiev, I.S., Soto, C., Gorman, J., Huang, J., Acharya, P., Chuang, G., Ofek, G., et al. (2014). Structure and immune recognition of trimeric pre-fusion HIV-1 Env. Nature *514*, 455–461.

Peden, K., Emerman, M., and Montagnier, L. (1991). Changes in growth properties on passage in tissue culture of viruses derived from infectious molecular clones of HIV-1LAI, HIV-1MAL, and HIV-1ELI. Virology *185*, 661–672.

Penczek, P.A., Grassucci, R.A., and Frank, J. (1994). The ribosome at improved resolution: New techniques for merging and orientation refinement in 3D cryo-electron microscopy of biological particles. Ultramicroscopy *53*, 251–270.

Petoukhov, M. V., Konarev, P. V., Kikhney, A.G., and Svergun, D.I. (2007). ATSAS 2.1 - Towards automated and web-supported small-angle scattering data analysis. J. Appl. Crystallogr. *40*, 223–228.

Pugach, P., Ozorowski, G., Cupo, A., Ringe, R., Yasmeen, A., de Val, N., Derking, R., Kim, H.J., Korzun, J., Golabek, M., et al. (2015). A native-like SOSIP.664 trimer based on a HIV-1 subtype B env gene. J. Virol. *89*, 3380–3395.

Sanders, R.W., Vesanen, M., Schuelke, N., Master, A., Schiffner, L., Kalyanaraman, R., Paluch, M., Berkhout, B., Maddon, P.J., Olson, W.C., et al. (2002). Stabilization of the soluble, cleaved, trimeric form of the envelope glycoprotein complex of human immunodeficiency virus type 1. J. Virol. *76*, 8875–8889.

Sanders, R.W., Derking, R., Cupo, A., Julien, J.P., Yasmeen, A., de Val, N., Kim, H.J., Blattner, C., de la Peña, A.T., Korzun, J., et al. (2013). A next-generation cleaved, soluble HIV-1 Env trimer, BG505 SOSIP.664 gp140, expresses multiple epitopes for broadly neutralizing but not non-neutralizing antibodies. PLoS Pathog. *9*, e1003618.

Sanders, R.W., van Gils, M.J., Derking, R., Sok, D., Ketas, T.J., Burger, J.A., Ozorowski, G., Cupo, A., Simonich, C., Goo, L., et al. (2015). HIV-1 neutralizing antibodies induced by native-like envelope trimers. Science *349*, aac4223.

Schrodinger LLC (2010). The PyMOL molecular graphics system, version 1.3r1.

Schülke, N., Vesanen, M.S., Sanders, R.W., Zhu, P., Lu, M., Anselma, D.J., Villa, A.R., Parren, P.W.H.I., Binley, J.M., Roux, K.H., et al. (2002). Oligomeric and conformational properties of a proteolytically mature, disulfide-stabilized human immunodeficiency virus type 1 gp140 envelope glycoprotein. J. Virol. *76*, 7760–7776.

Smolsky, I.L., Liu, P., Niebuhr, M., Ito, K., Weiss, T.M., and Tsuruta, H. (2007). Biological small-angle X-ray scattering facility at the Stanford Synchrotron Radiation Laboratory. J. Appl. Crystallogr. *40*, 453–458.

Sok, D., van Gils, M.J., Pauthner, M., Julien, J., Saye-Francisco, K.L., Hsueh, J., Briney, B., Lee, J.H., Le, K.M., Lee, P.S., et al. (2014). Recombinant HIV envelope trimer selects for quaternary-dependent antibodies targeting the trimer apex. Proc. Natl. Acad. Sci. *111*, 17624–17629.

Svergun, D.I. (1992). Determination of the regularization parameter in indirect-transform methods using perceptual criteria. J. Appl. Crystallogr. *25*, 495–503.

Tang, G., Peng, L., Baldwin, P.R., Mann, D.S., Jiang, W., Rees, I., and Ludtke, S.J. (2007). EMAN2: an extensible image processing suite for electron microscopy. J. Struct. Biol. *157*, 38–46.

Yasmeen, A., Ringe, R., Derking, R., Cupo, A., Julien, J.-P., Burton, D.R., Ward, A.B., Wilson, I. a, Sanders, R.W., Moore, J.P., et al. (2014). Differential binding of neutralizing and non-neutralizing antibodies to native-like soluble HIV-1 Env trimers, uncleaved Env proteins, and monomeric subunits. Retrovirology *11*, 41.

Figure S1

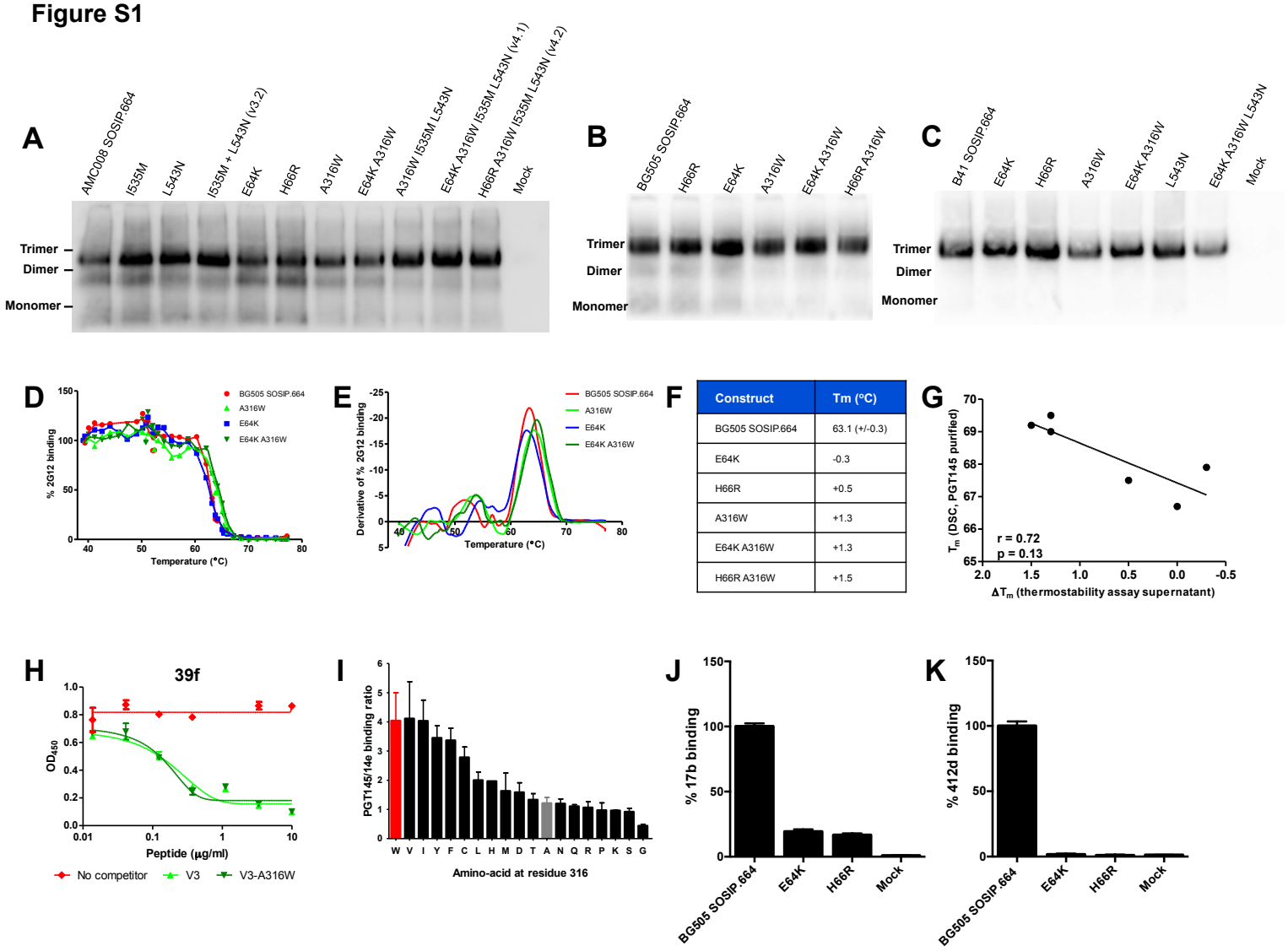
A
AMC008 SOSIP.664
I535M
L543N
I535M + L543N (v3.2)
E64K
H66R
A316W
E64K A316W
A316W I535M L543N
E64K A316W I535M L543N (v4.1)
H66R A316W I535M L543N (v4.2)
Mock
Trimer
Dimer
Monomer
B
BG505 SOSIP.664
H66R
E64K
A316W
E64K A316W
H66R A316W
Trimer
Dimer
Monomer
C
B41 SOSIP.664
E64K
H66R
A316W
E64K A316W
L543N
E64K A316W L543N
Mock
Trimer
Dimer
Monomer
D
% 2G12 binding
Temperature (°C)
BG505 SOSIP.664
A316W
E64K
E64K A316W
E
Derivative of % 2G12 binding
Temperature (°C)
BG505 SOSIP.664
A316W
E64K
E64K A316W
F
Construct
Tm (°C)
BG505 SOSIP.664
63.1 (+/-0.3)
E64K
-0.3
H66R
+0.5
A316W
+1.3
E64K A316W
+1.3
H66R A316W
+1.5
G
Tm (DSC, PGT145 purified)
ΔTm (thermostability assay supernatant)
r = 0.72
p = 0.13
H
39f
OD450
Peptide (µg/ml)
No competitor
V3
V3-A316W
I
PGT145/14e binding ratio
W V I Y F C L H M D T A N Q R P K S G
Amino-acid at residue 316
J
% 17b binding
BG505 SOSIP.664
E64K
H66R
Mock
K
% 412d binding
BG505 SOSIP.664
E64K
H66R
Mock

Figure S2

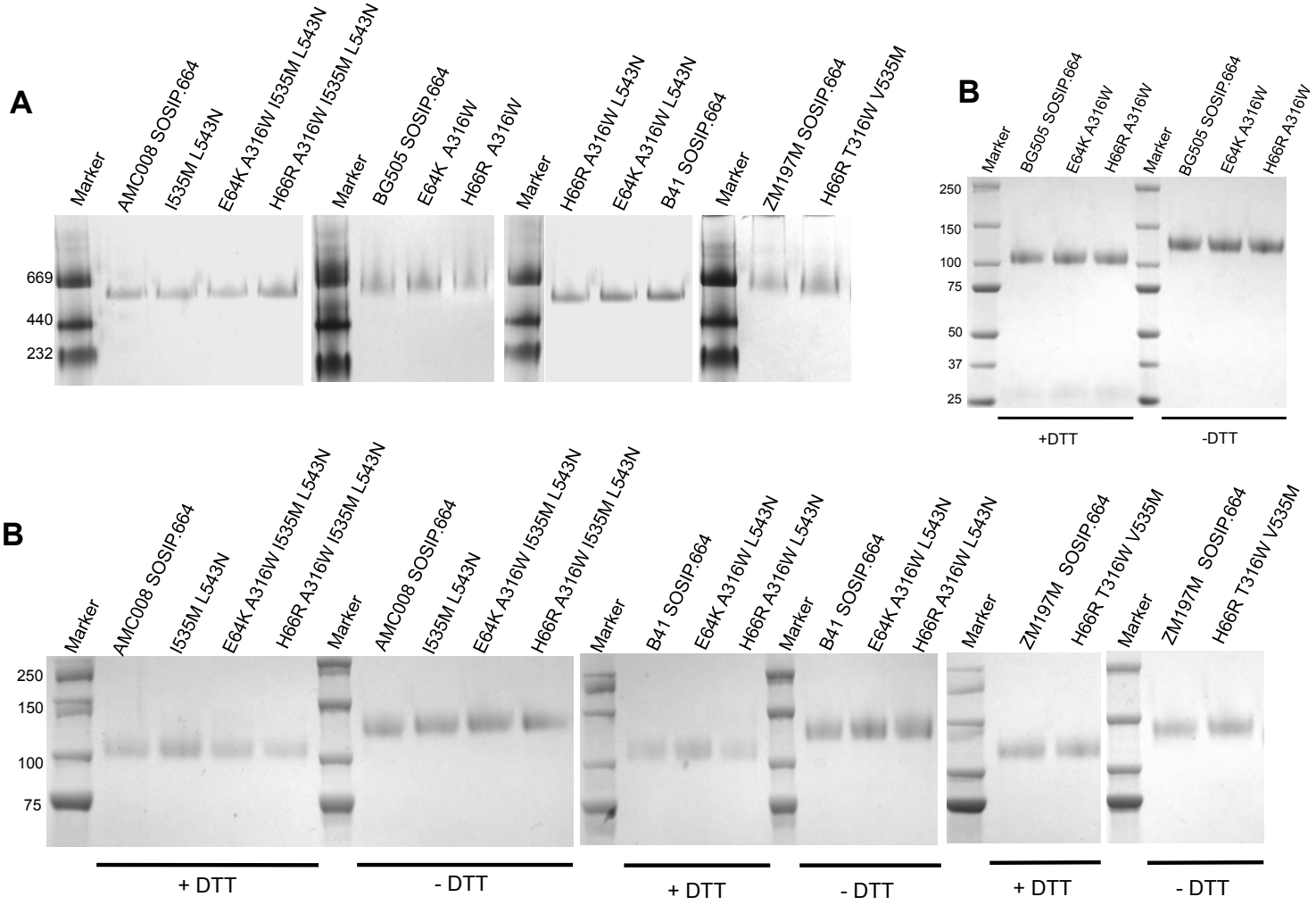

C

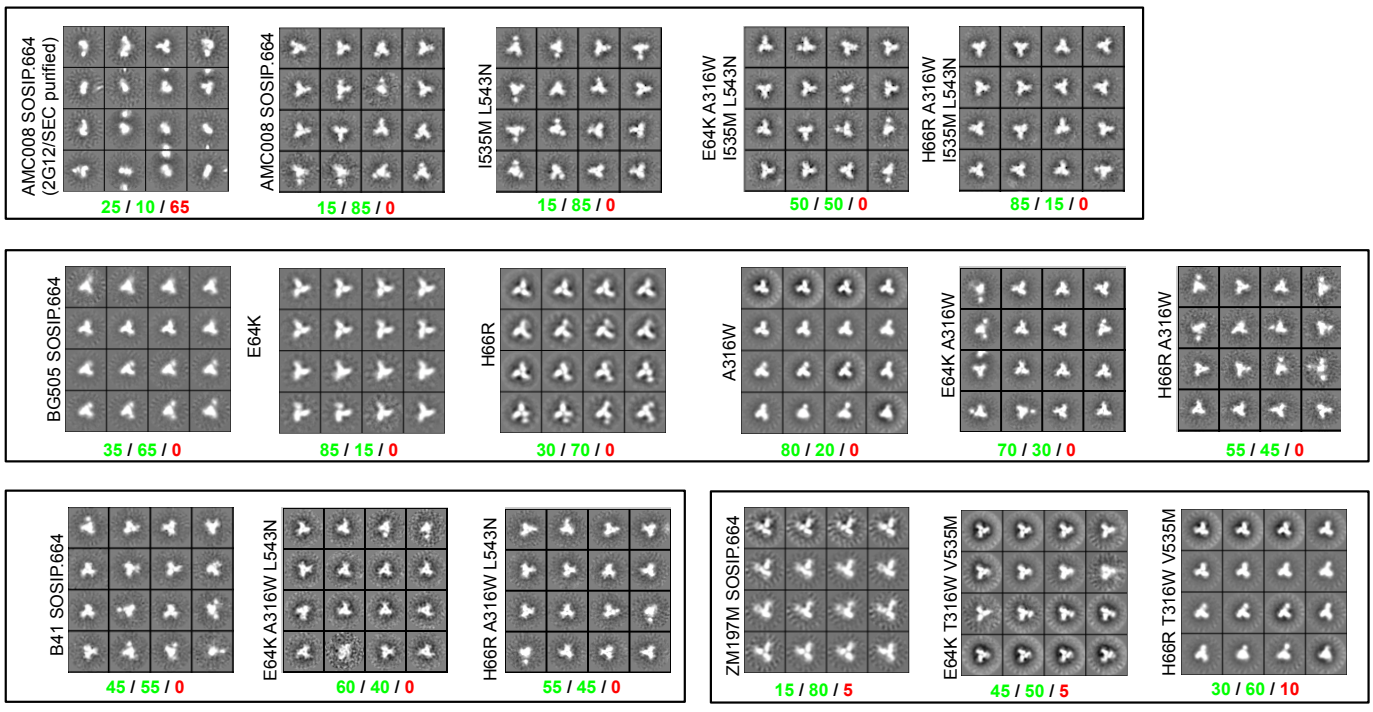

Percentage closed / open / non native like trimers

Figure S3

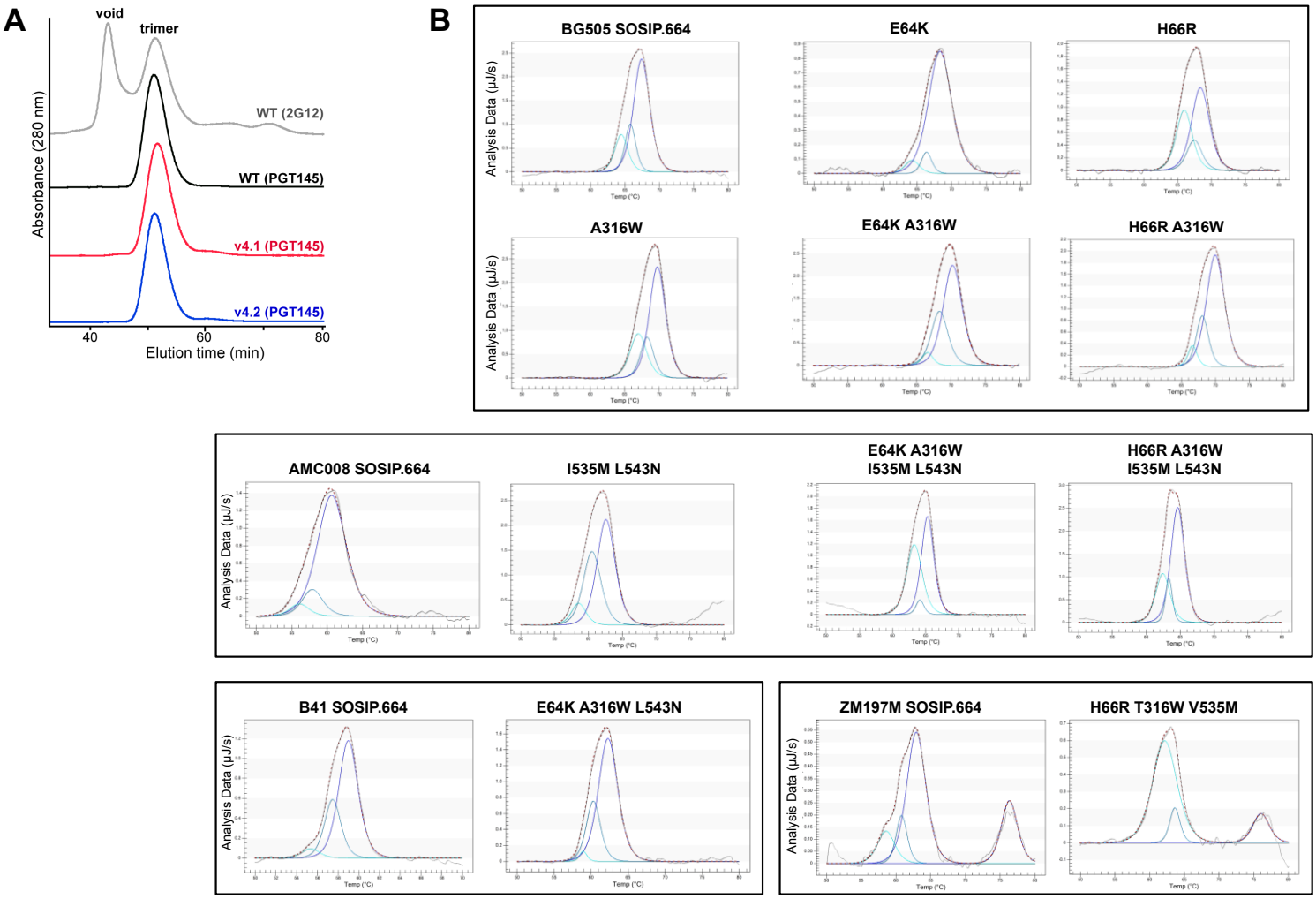

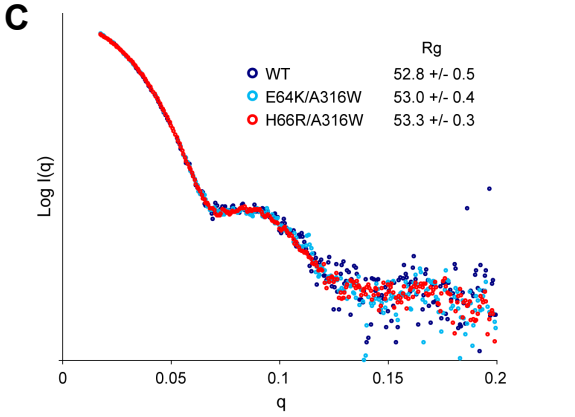

	DLS		SAXS	
	R_h (Å)	Poly dispersity %	R_g (Å) Guinier	R_g (Å) GNOM
BG505 SOSIP.664	69.1	3.8	52.8	52.5
E64K A316W	68.7	3.3	53.0	51.9
H66R A316W	68.6	2.2	53.3	51.7

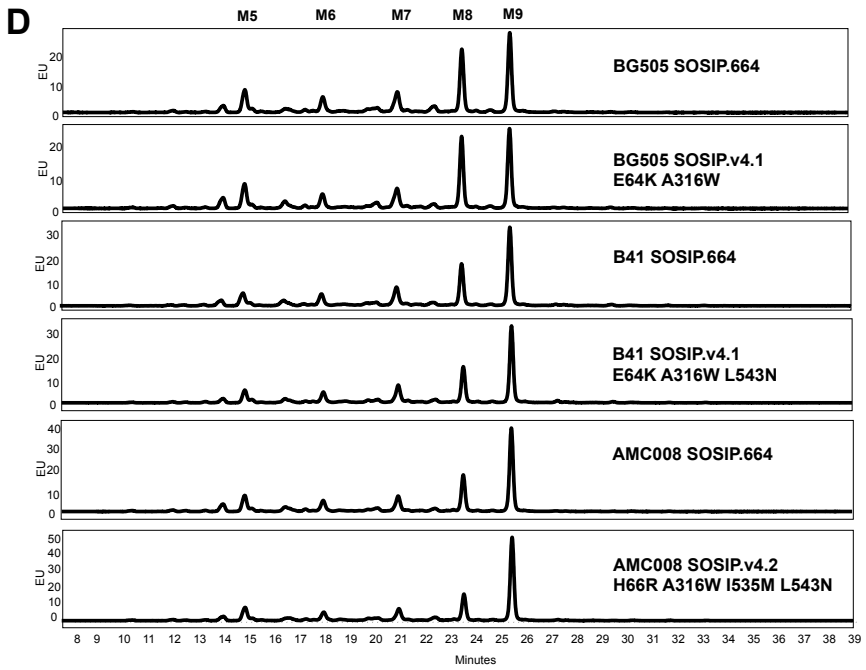

Figure S4

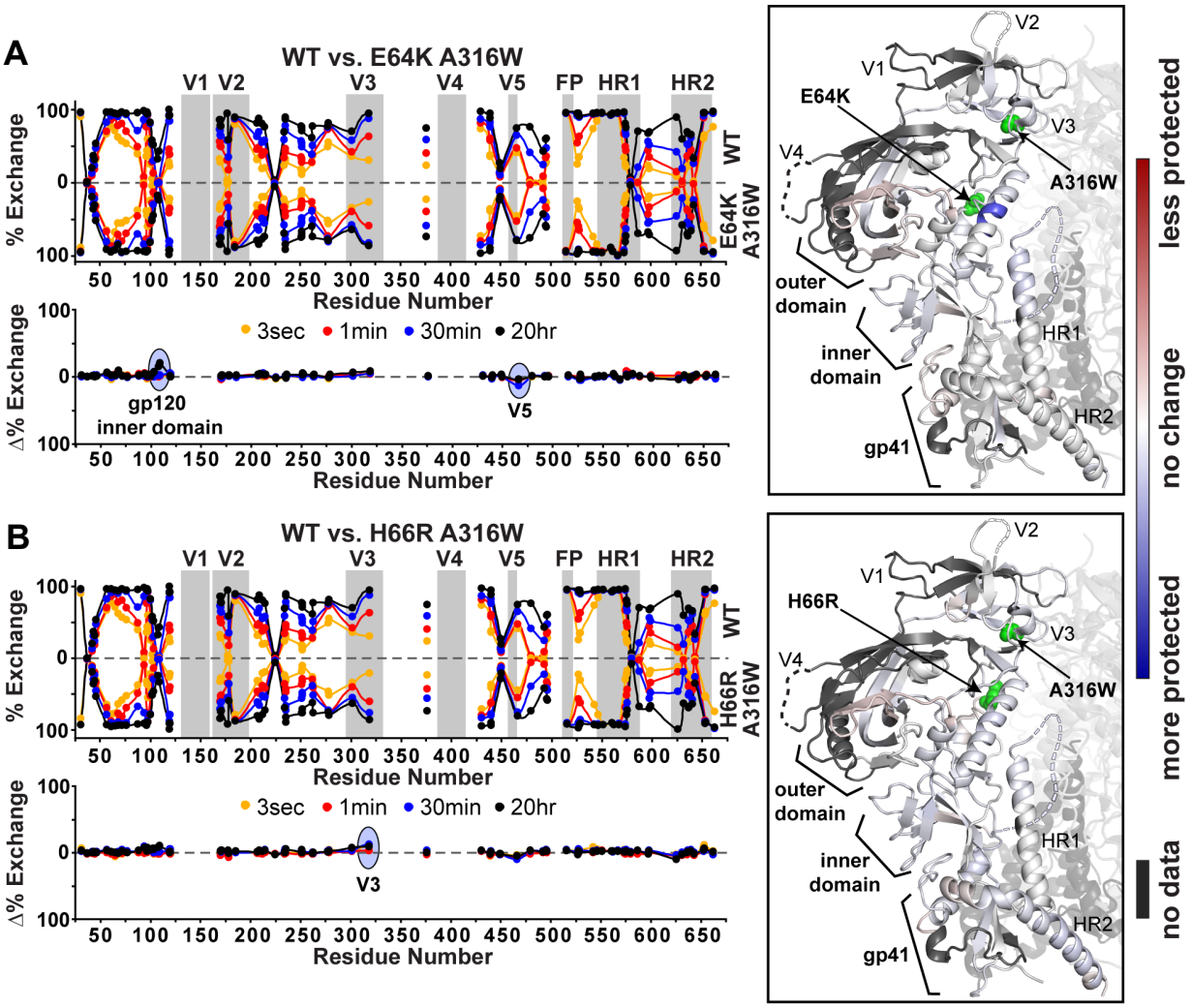
A
WT vs. E64K A316W
V1 V2
V3
V4
V5
FP
HR1
HR2
% Exchange
WT
E64K A316W
Residue Number
3sec
1min
30min
20hr
Δ% Exchange
gp120 inner domain
V5
B
WT vs. H66R A316W
H66R A316W
V3
E64K
H66R
A316W
outer domain
inner domain
HR1
HR2
gp41
less protected
no change
more protected
no data

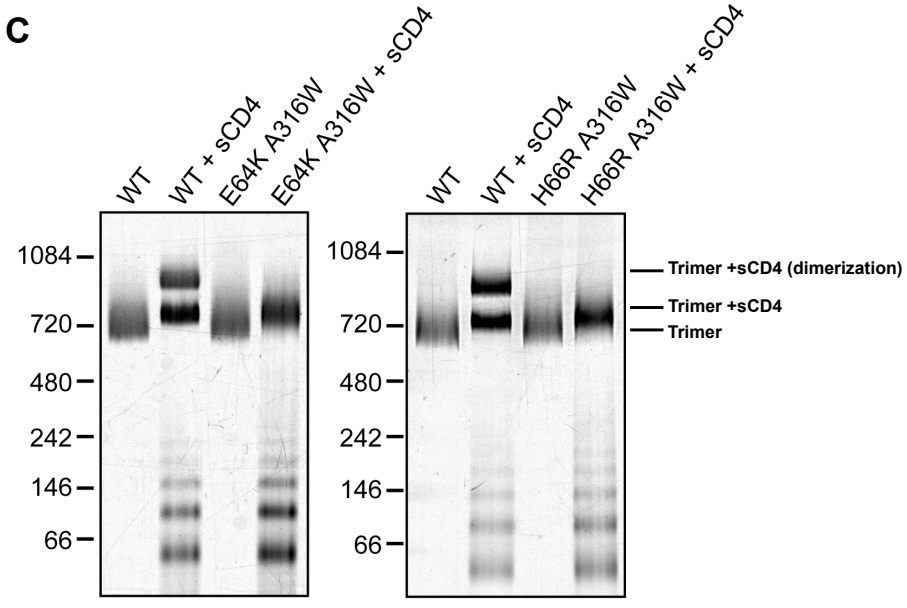
C
WT
WT + sCD4
E64K A316W
E64K A316W + sCD4
H66R A316W
H66R A316W + sCD4
1084
720
480
242
146
66
Trimer +sCD4 (dimerization)
Trimer +sCD4
Trimer

Figure S5

A

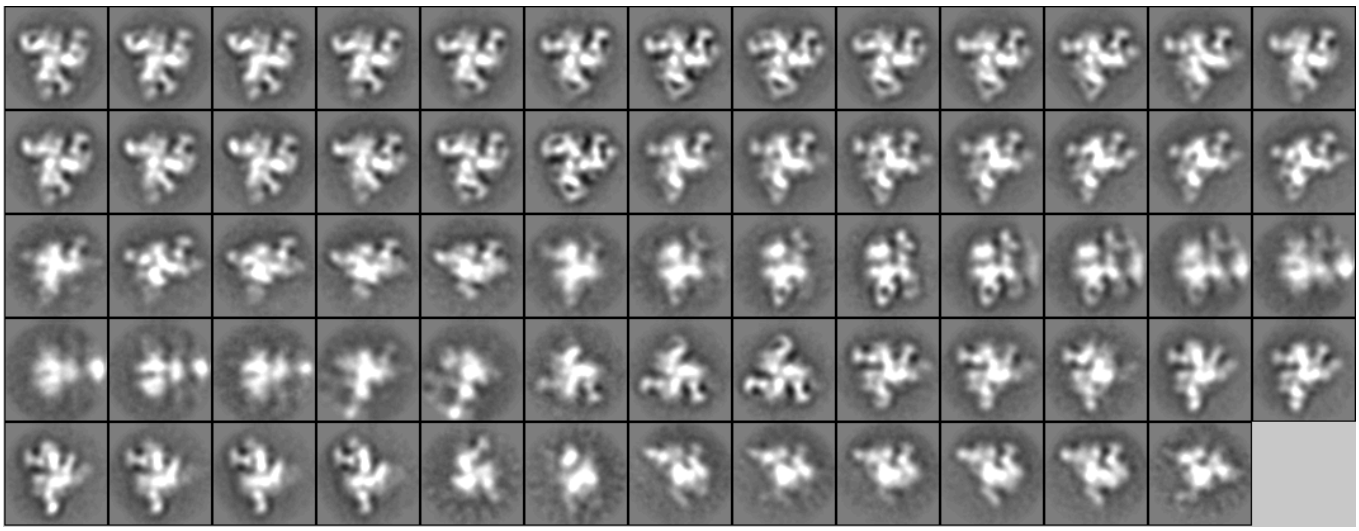

B

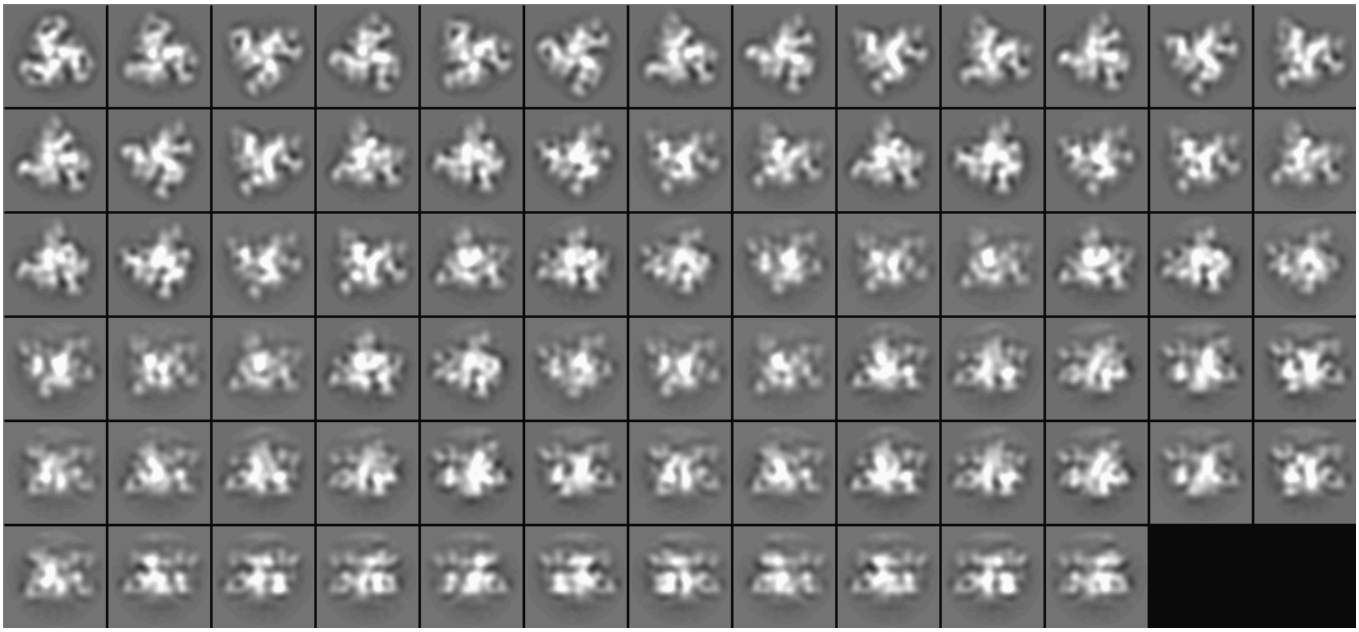

C

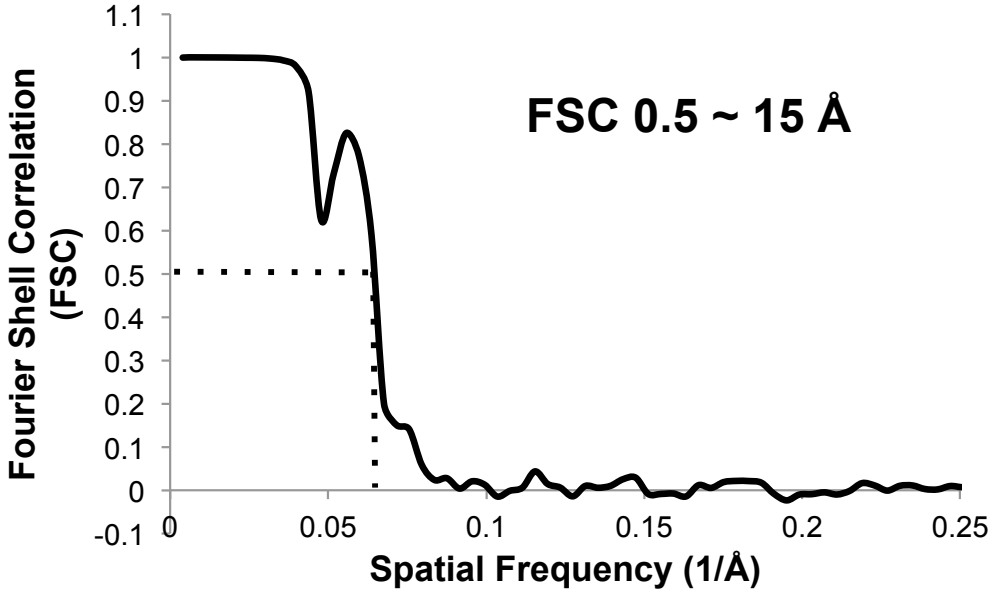

Figure S6

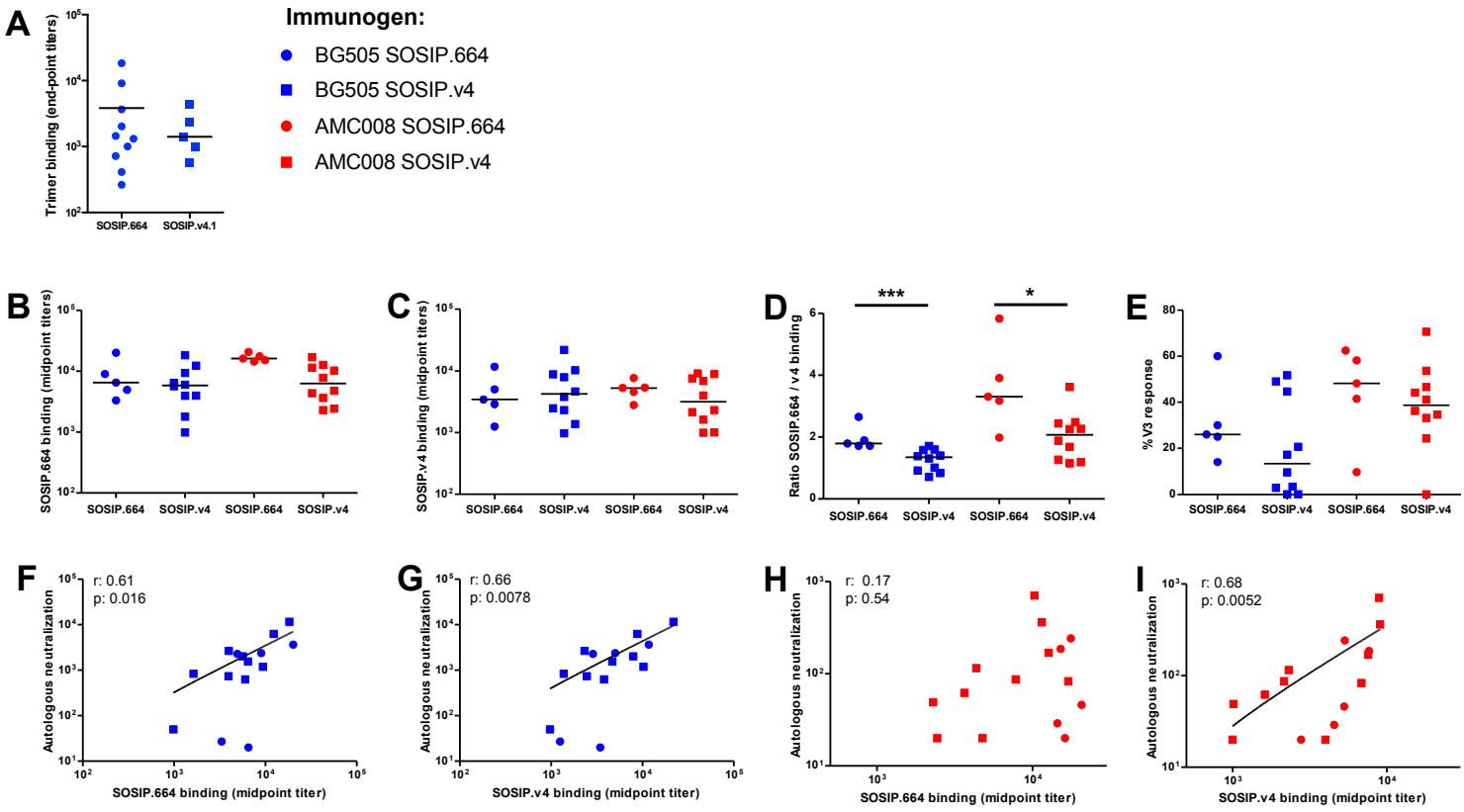
A
Trimer binding (end-point titers)
SOSIP.664
SOSIP.v4.1
Immunogen:
BG505 SOSIP.664
BG505 SOSIP.v4
AMC008 SOSIP.664
AMC008 SOSIP.v4
B
SOSIP.664 binding (midpoint titers)
C
SOSIP.v4 binding (midpoint titers)
D
Ratio SOSIP.664 / v4 binding
***
*
E
% V3 response
F
r: 0.61
p: 0.016
Autologous neutralization
SOSIP.664 binding (midpoint titer)
G
r: 0.66
p: 0.0078
SOSIP.v4 binding (midpoint titer)
H
r: 0.17
p: 0.54
I
r: 0.68
p: 0.0052

Data S1

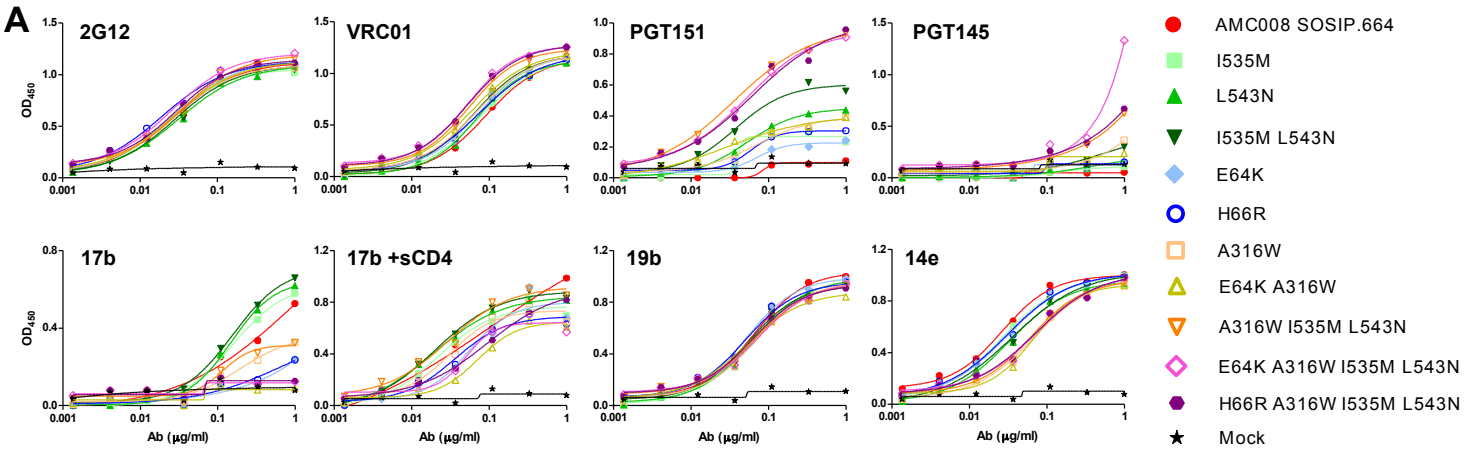
A
2G12
VRC01
PGT151
PGT145
17b
17b +sCD4
19b
14e
OD450
Ab (µg/ml)
AMC008 SOSIP.664
I535M
L543N
I535M L543N
E64K
H66R
A316W
E64K A316W
A316W I535M L543N
E64K A316W I535M L543N
H66R A316W I535M L543N
Mock

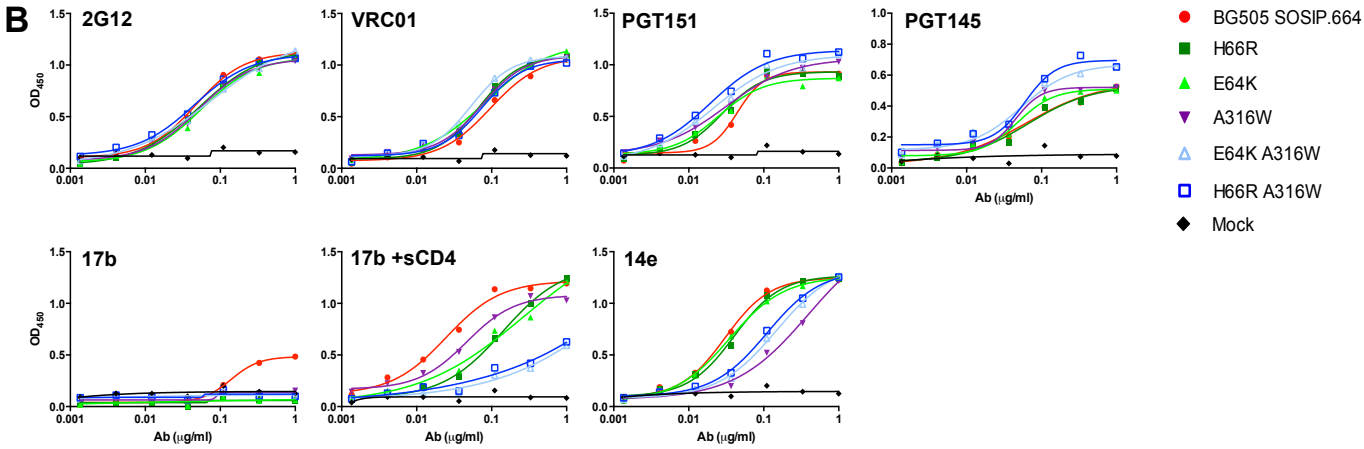
B
2G12
VRC01
PGT151
PGT145
17b
17b +sCD4
14e
OD450
Ab (µg/ml)
BG505 SOSIP.664
H66R
E64K
A316W
E64K A316W
H66R A316W
Mock

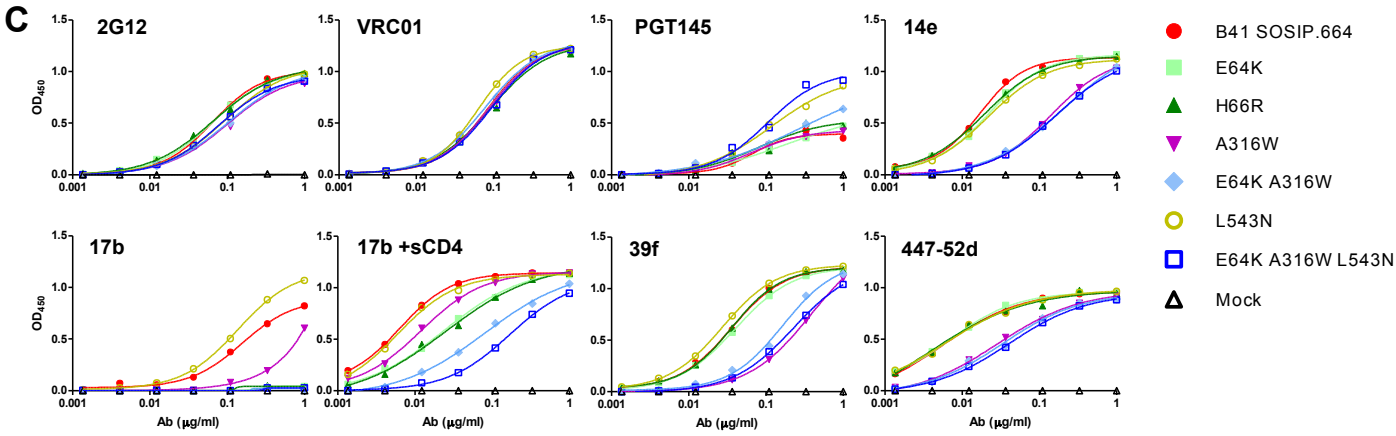
C
2G12
VRC01
PGT145
14e
17b
17b +sCD4
39f
447-52d
OD450
Ab (µg/ml)
B41 SOSIP.664
E64K
H66R
A316W
E64K A316W
L543N
E64K A316W L543N
Mock

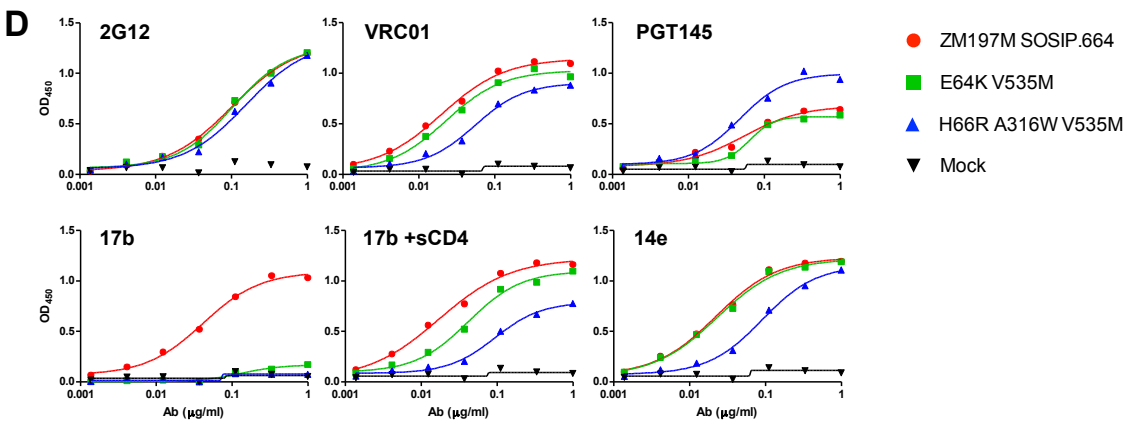
D
2G12
VRC01
PGT145
17b
17b +sCD4
14e
OD450
Ab (µg/ml)
ZM197M SOSIP.664
E64K V535M
H66R A316W V535M
Mock

Data S1

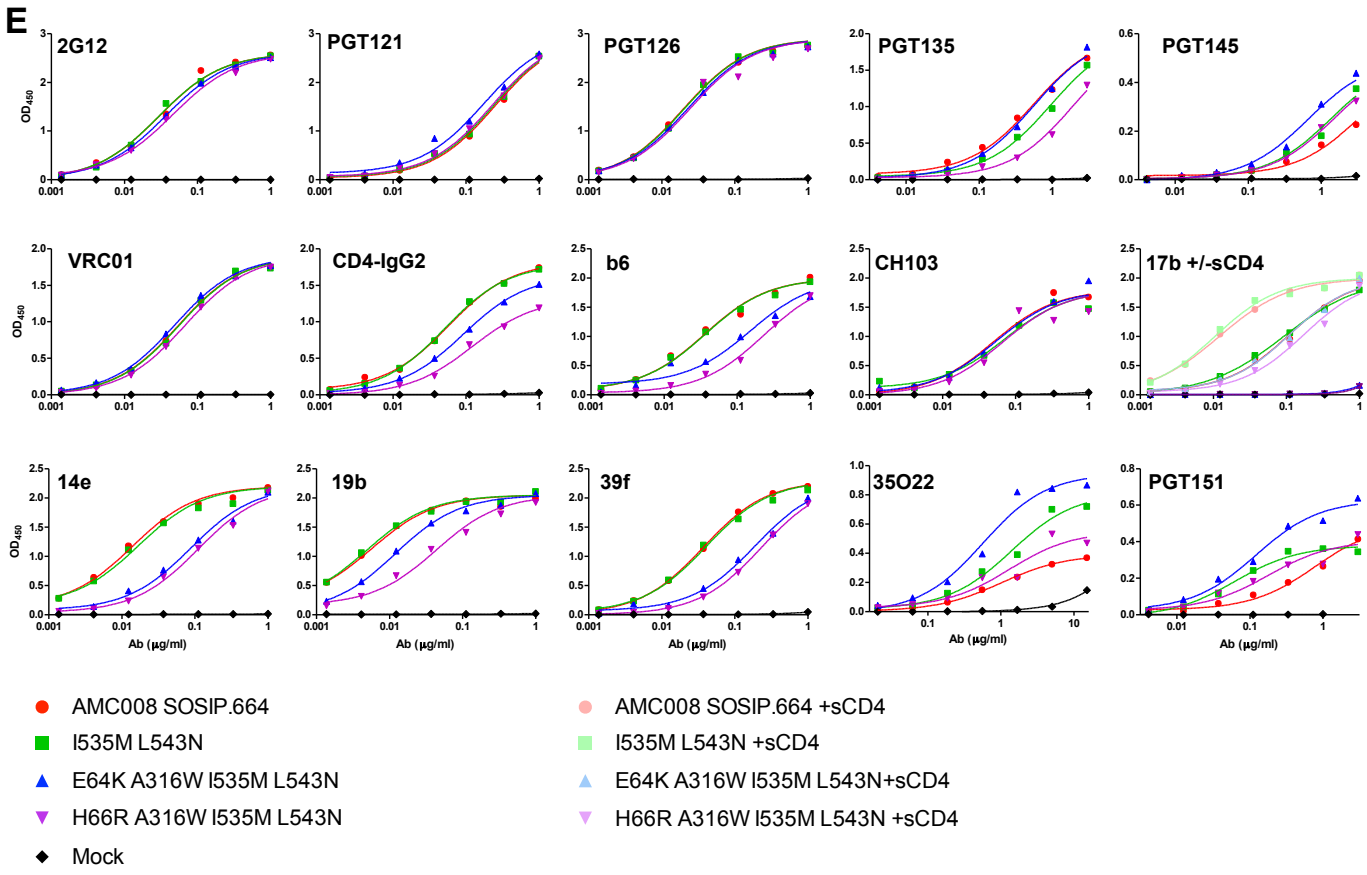
E
2G12
PGT121
PGT126
PGT135
PGT145
VRC01
CD4-IgG2
b6
CH103
17b +/-sCD4
14e
19b
39f
35O22
PGT151
OD450
Ab (µg/ml)
AMC008 SOSIP.664
I535M L543N
E64K A316W I535M L543N
H66R A316W I535M L543N
Mock
AMC008 SOSIP.664 +sCD4
I535M L543N +sCD4
E64K A316W I535M L543N+sCD4
H66R A316W I535M L543N +sCD4

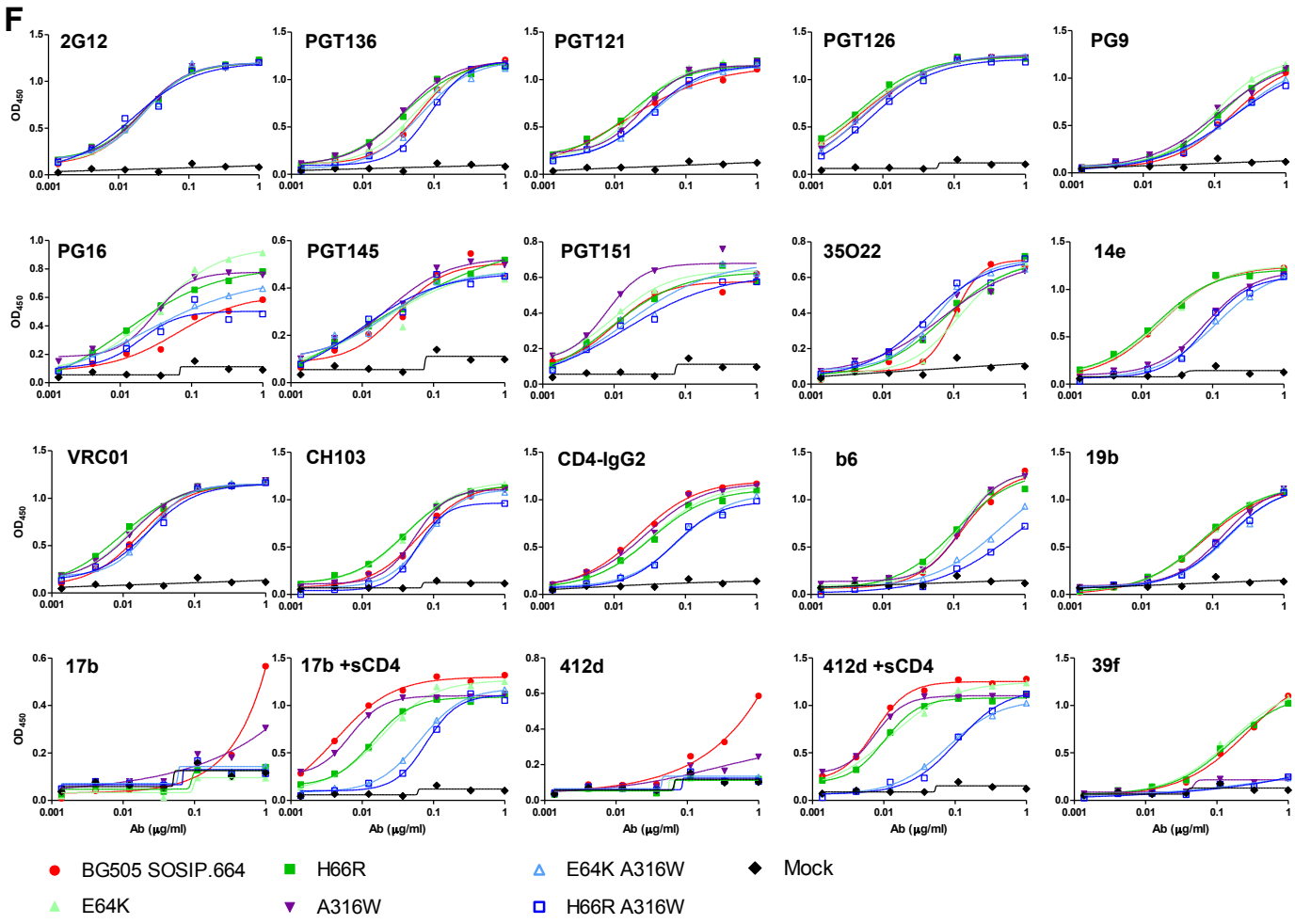
F
2G12
PGT136
PGT121
PGT126
PG9
PG16
PGT145
PGT151
35O22
14e
VRC01
CH103
CD4-IgG2
b6
19b
17b
17b +sCD4
412d
412d +sCD4
39f
OD450
Ab (µg/ml)
BG505 SOSIP.664
H66R
E64K A316W
Mock
E64K
A316W
H66R A316W

Data S1

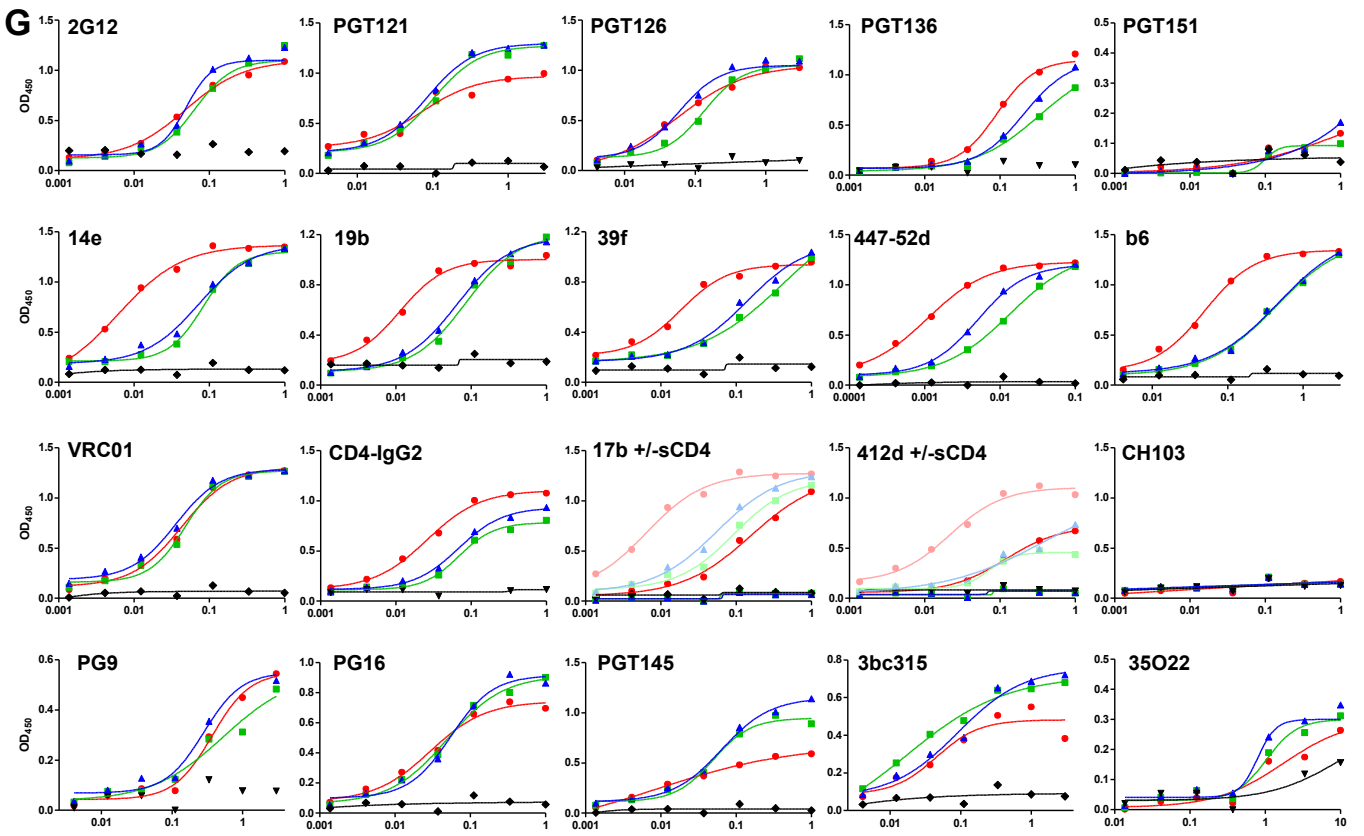
G
2G12
PGT121
PGT126
PGT136
PGT151
14e
19b
39f
447-52d
b6
VRC01
CD4-IgG2
17b +/-sCD4
412d +/-sCD4
CH103
PG9
PG16
PGT145
3bc315
35O22
OD450
B41 SOSIP.664
E64K A316W L543N
H66R A316W L543N
B41 SOSIP.664 +sCD4
E64K A316W L543N +sCD4
H66R A316W L543N +sCD4
Mock

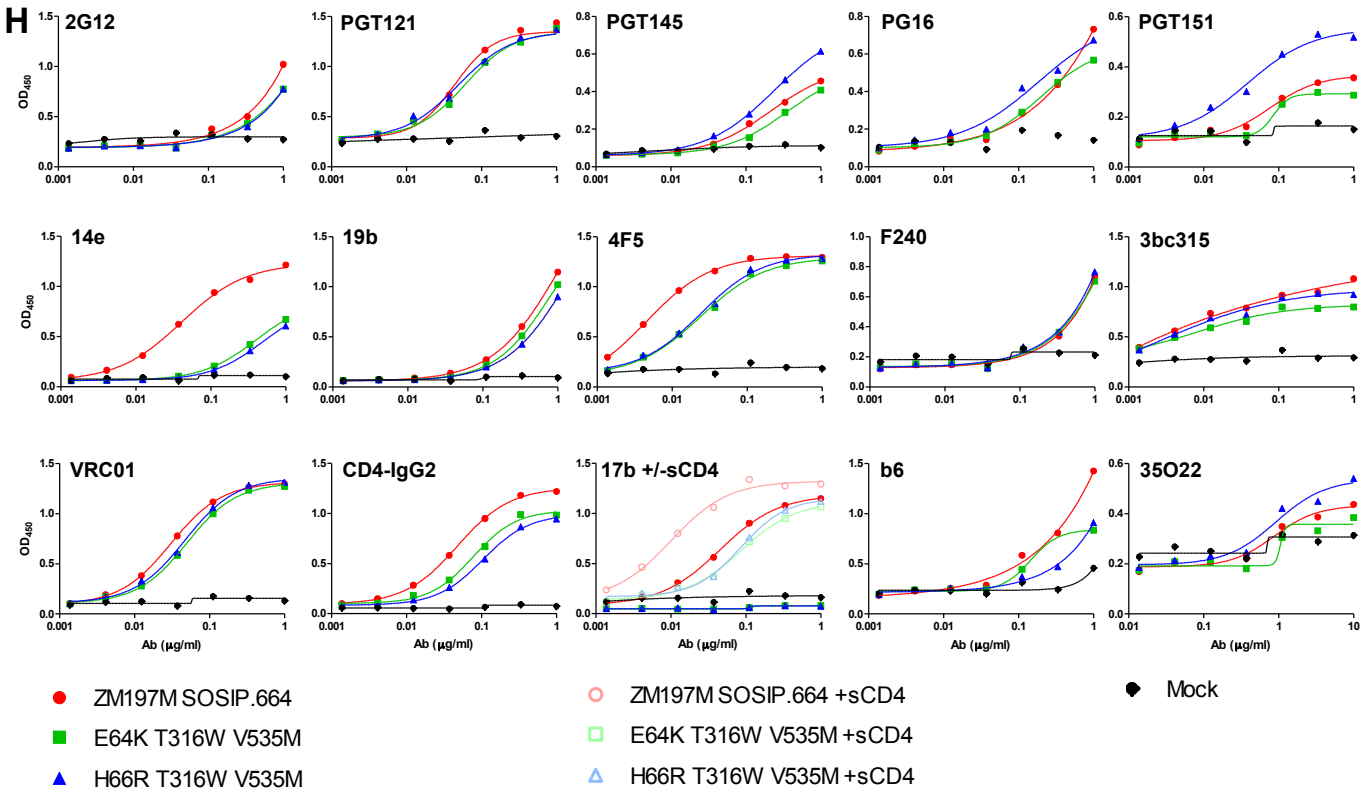
H
2G12
PGT121
PGT145
PG16
PGT151
14e
19b
4F5
F240
3bc315
VRC01
CD4-IgG2
17b +/-sCD4
b6
35O22
OD450
Ab (µg/ml)
ZM197M SOSIP.664
E64K T316W V535M
H66R T316W V535M
ZM197M SOSIP.664 +sCD4
E64K T316W V535M +sCD4
H66R T316W V535M +sCD4
Mock

Data S1

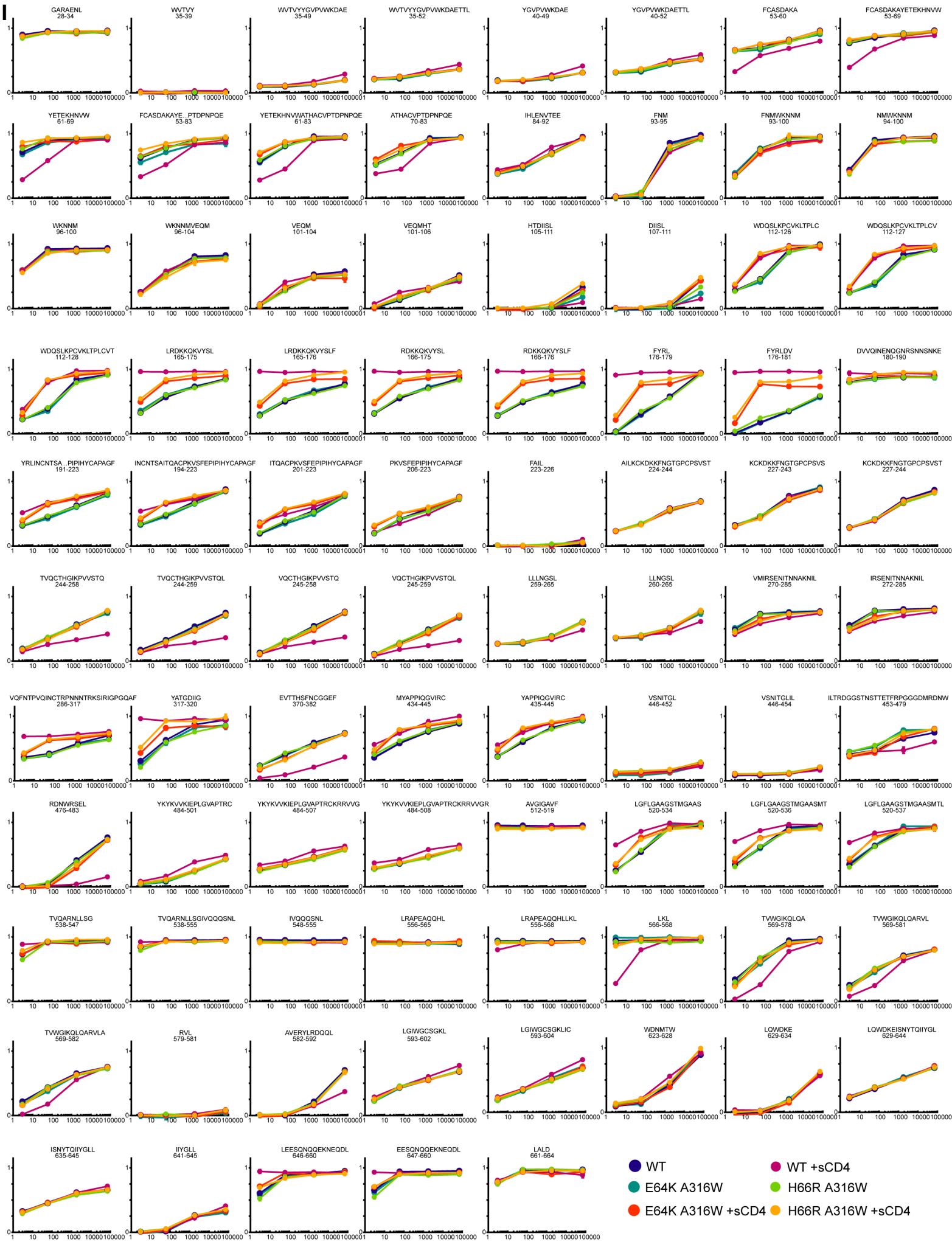
GARAENL
28-34
WVTVY
35-39
WVTVYYGVPVWKDAE
35-49
WVTVYYGVPVWKDAETTL
35-52
YGVPVWKDAE
40-49
YGVPVWKDAETTL
40-52
FCASDAKA
53-60
FCASDAKAYETEKHNVW
53-69
YETEKHNVW
61-69
FCASDAKAYE...PTDPNPQE
53-83
YETEKHNVWATHACVPTDPNPQE
61-83
ATHACVPTDPNPQE
70-83
IHLENVTEE
84-92
FNM
93-95
FNMWKNNM
93-100
NMWKNNM
94-100
WKNNM
96-100
WKNNMVEQM
96-104
VEQM
101-104
VEQMHT
101-106
HTDIISL
105-111
DIISL
107-111
WDQSLKPCVKLTPLC
112-126
WDQSLKPCVKLTPLCV
112-127
WDQSLKPCVKLTPLCVT
112-128
LRDKKQKVYSL
165-175
LRDKKQKVYSLF
165-176
RDKKQKVYSL
166-175
RDKKQKVYSLF
166-176
FYRL
176-179
FYRLDV
176-181
DVVQINENQGNRSNNSNKE
180-190
YRLINCNTSA...PIPIHYCAPAGF
191-223
INCNTSAITQACPKVSFEPIPIHYCAPAGF
194-223
ITQACPKVSFEPIPIHYCAPAGF
201-223
PKVSFEPIPIHYCAPAGF
206-223
FAIL
223-226
AILKCKDKKFNGTGPCPSVST
224-244
KCKDKKFNGTGPCPSVS
227-243
KCKDKKFNGTGPCPSVST
227-244
TVQCTHGIKPVVSTQ
244-258
TVQCTHGIKPVVSTQL
244-259
VQCTHGIKPVVSTQ
245-258
VQCTHGIKPVVSTQL
245-259
LLLNGSL
259-265
LLNGSL
260-265
VMIRSENITNNAKNIL
270-285
IRSENITNNAKNIL
272-285
VQFNTPVQINCTRPNNNTRKSIRIGPGQAF
286-317
YATGDIIG
317-320
EVTTHSFNCGGEF
370-382
MYAPPIQGVIRC
434-445
YAPPIQGVIRC
435-445
VSNITGL
446-452
VSNITGLIL
446-454
ILTRDGGSTNSTTETFRPGGGDMRDNW
453-479
RDNWRSEL
476-483
YKYKVVKIEPLGVAPTRC
484-501
YKYKVVKIEPLGVAPTRCKRRVVG
484-507
YKYKVVKIEPLGVAPTRCKRRVVGR
484-508
AVGIGAVF
512-519
LGFLGAAGSTMGAAS
520-534
LGFLGAAGSTMGAASMT
520-536
LGFLGAAGSTMGAASMTL
520-537
TVQARNLLSG
538-547
TVQARNLLSGIVQQQSNL
538-555
IVQQQSNL
548-555
LRAPEAQQHL
556-565
LRAPEAQQHLLKL
556-568
LKL
566-568
TVWGIKQLQA
569-578
TVWGIKQLQARVL
569-581
TVWGIKQLQARVLA
569-582
RVL
579-581
AVERYLRDQQL
582-592
LGIWGCSGKL
593-602
LGIWGCSGKLIC
593-604
WDNMTW
623-628
LQWDKE
629-634
LQWDKEISNYTQIIYGL
629-644
ISNYTQIIYGLL
635-645
IIYGLL
641-645
LEESQNQQEKNEQDL
646-660
EESQNQQEKNEQDL
647-660
LALD
661-664
WT
WT +sCD4
E64K A316W
H66R A316W
E64K A316W +sCD4
H66R A316W +sCD4